astro-ph 1111.2735

arXiv:1111.2735v2 [astro-ph.HE] 23 Nov 2011

32ND INTERNATIONAL COSMIC RAY CONFERENCE, BEIJING 2011

The IceCube Neutrino Observatory III: Cosmic Rays

THE ICECUBE COLLABORATION

1. The IceTop Air Shower Array: Detector Overview, Physics Goals and First Result **1**

2. Cosmic Ray Composition from the 40-string IceCube/IceTop Detectors **5**

3. Seasonal Variations of High Energy Cosmic Ray Muons Observed by the IceCube Observatory as a Probe of Kaon/Pion Ratio **9**

4. Measurements of the Air Shower Parameters with IceTop **13**

5. Extensive Air Showers Measured by the 79-string IceCube Observatory at South Pole **17**

6. Simulation of IceTop VEM calibration and the dependency on the snow layer **21**

7. Atmospheric Muon Spectrum from Catastrophic Energy Losses in IceCube **25**

8. Study of High p_T Muons in IceCube **29**

9. Searching for PeV gamma rays with IceCube **33**

10. Energy Dependence of the Large Scale Galactic Cosmic Rays Anisotropy Measured With IceCube **37**

11. Observation of Anisotropy in the Arrival Direction Distribution of Cosmic Rays at TeV Energies with IceCube **41**

12. Measurement of the Solar Anisotropy with IceCube **45**

13. Study of Forbush Decreases with IceTop **49**

32ND INTERNATIONAL COSMIC RAY CONFERENCE, BEIJING 2011

IceCube Collaboration Member List

R. ABBASI[28], Y. ABDOU[22], T. ABU-ZAYYAD[33], M. ACKERMANN[39], J. ADAMS[16], J. A. AGUILAR[28], M. AHLERS[32], M. M. ALLEN[36], D. ALTMANN[1], K. ANDEEN[28,a], J. AUFFENBERG[38], X. BAI[31,b], M. BAKER[28], S. W. BARWICK[24], R. BAY[7], J. L. BAZO ALBA[39], K. BEATTIE[8], J. J. BEATTY[18,19], S. BECHET[13], J. K. BECKER[10], K.-H. BECKER[38], M. L. BENABDERRAHMANE[39], S. BENZVI[28], J. BERDERMANN[39], P. BERGHAUS[31], D. BERLEY[17], E. BERNARDINI[39], D. BERTRAND[13], D. Z. BESSON[26], D. BINDIG[38], M. BISSOK[1], E. BLAUFUSS[17], J. BLUMENTHAL[1], D. J. BOERSMA[1], C. BOHM[34], D. BOSE[14], S. BÖSER[11], O. BOTNER[37], A. M. BROWN[16], S. BUITINK[14], K. S. CABALLERO-MORA[36], M. CARSON[22], D. CHIRKIN[28], B. CHRISTY[17], F. CLEVERMANN[20], S. COHEN[25], C. COLNARD[23], D. F. COWEN[36,35], A. H. CRUZ SILVA[39], M. V. D'AGOSTINO[7], M. DANNINGER[34], J. DAUGHHETEE[5], J. C. DAVIS[18], C. DE CLERCQ[14], T. DEGNER[11], L. DEMIRÖRS[25], F. DESCAMPS[22], P. DESIATI[28], G. DE VRIES-UITERWEERD[22], T. DEYOUNG[36], J. C. DÍAZ-VÉLEZ[28], M. DIERCKXSENS[13], J. DREYER[10], J. P. DUMM[28], M. DUNKMAN[36], J. EISCH[28], R. W. ELLSWORTH[17], O. ENGDEGÅRD[37], S. EULER[1], P. A. EVENSON[31], O. FADIRAN[28], A. R. FAZELY[6], A. FEDYNITCH[10], J. FEINTZEIG[28], T. FEUSELS[22], K. FILIMONOV[7], C. FINLEY[34], T. FISCHER-WASELS[38], B. D. FOX[36], A. FRANCKOWIAK[11], R. FRANKE[39], T. K. GAISSER[31], J. GALLAGHER[27], L. GERHARDT[8,7], L. GLADSTONE[28], T. GLÜSENKAMP[39], A. GOLDSCHMIDT[8], J. A. GOODMAN[17], D. GÓRA[39], D. GRANT[21], T. GRIESEL[29], A. GROSS[16,23], S. GRULLON[28], M. GURTNER[38], C. HA[36], A. HAJ ISMAIL[22], A. HALLGREN[37], F. HALZEN[28], K. HAN[39], K. HANSON[13,28], D. HEINEN[1], K. HELBING[38], R. HELLAUER[17], S. HICKFORD[16], G. C. HILL[28], K. D. HOFFMAN[17], A. HOMEIER[11], K. HOSHINA[28], W. HUELSNITZ[17,c], J.-P. HÜLSS[1], P. O. HULTH[34], K. HULTQVIST[34], S. HUSSAIN[31], A. ISHIHARA[15], E. JACOBI[39], J. JACOBSEN[28], G. S. JAPARIDZE[4], H. JOHANSSON[34], K.-H. KAMPERT[38], A. KAPPES[9], T. KARG[38], A. KARLE[28], P. KENNY[26], J. KIRYLUK[8,7], F. KISLAT[39], S. R. KLEIN[8,7], J.-H. KÖHNE[20], G. KOHNEN[30], H. KOLANOSKI[9], L. KÖPKE[29], S. KOPPER[38], D. J. KOSKINEN[36], M. KOWALSKI[11], T. KOWARIK[29], M. KRASBERG[28], T. KRINGS[1], G. KROLL[29], N. KURAHASHI[28], T. KUWABARA[31], M. LABARE[14], K. LAIHEM[1], H. LANDSMAN[28], M. J. LARSON[36], R. LAUER[39], J. LÜNEMANN[29], J. MADSEN[33], A. MAROTTA[13], R. MARUYAMA[28], K. MASE[15], H. S. MATIS[8], K. MEAGHER[17], M. MERCK[28], P. MÉSZÁROS[35,36], T. MEURES[13], S. MIARECKI[8,7], E. MIDDELL[39], N. MILKE[20], J. MILLER[37], T. MONTARULI[28,d], R. MORSE[28], S. M. MOVIT[35], R. NAHNHAUER[39], J. W. NAM[24], U. NAUMANN[38], D. R. NYGREN[8], S. ODROWSKI[23], A. OLIVAS[17], M. OLIVO[10], A. O'MURCHADHA[28], S. PANKNIN[11], L. PAUL[1], C. PÉREZ DE LOS HEROS[37], J. PETROVIC[13], A. PIEGSA[29], D. PIELOTH[20], R. PORRATA[7], J. POSSELT[38], P. B. PRICE[7], G. T. PRZYBYLSKI[8], K. RAWLINS[3], P. REDL[17], E. RESCONI[23,e], W. RHODE[20], M. RIBORDY[25], M. RICHMAN[17], J. P. RODRIGUES[28], F. ROTHMAIER[29], C. ROTT[18], T. RUHE[20], D. RUTLEDGE[36], B. RUZYBAYEV[31], D. RYCKBOSCH[22], H.-G. SANDER[29], M. SANTANDER[28], S. SARKAR[32], K. SCHATTO[29], T. SCHMIDT[17], A. SCHÖNWALD[39], A. SCHUKRAFT[1], A. SCHULTES[38], O. SCHULZ[23,f], M. SCHUNCK[1], D. SECKEL[31], B. SEMBURG[38], S. H. SEO[34], Y. SESTAYO[23], S. SEUNARINE[12], A. SILVESTRI[24], G. M. SPICZAK[33], C. SPIERING[39], M. STAMATIKOS[18,g], T. STANEV[31], T. STEZELBERGER[8], R. G. STOKSTAD[8], A. STÖSSL[39], E. A. STRAHLER[14], R. STRÖM[37], M. STÜER[11], G. W. SULLIVAN[17], Q. SWILLENS[13], H. TAAVOLA[37], I. TABOADA[5], A. TAMBURRO[33], A. TEPE[5], S. TER-ANTONYAN[6], S. TILAV[31], P. A. TOALE[2], S. TOSCANO[28], D. TOSI[39], N. VAN EIJNDHOVEN[14], J. VANDENBROUCKE[7], A. VAN OVERLOOP[22], J. VAN SANTEN[28], M. VEHRING[1], M. VOGE[11], C. WALCK[34], T. WALDENMAIER[9], M. WALLRAFF[1], M. WALTER[39], CH. WEAVER[28], C. WENDT[28], S. WESTERHOFF[28], N. WHITEHORN[28], K. WIEBE[29], C. H. WIEBUSCH[1], D. R. WILLIAMS[2], R. WISCHNEWSKI[39], H. WISSING[17], M. WOLF[23], T. R. WOOD[21], K. WOSCHNAGG[7], C. XU[31], D. L. XU[2], X. W. XU[6], J. P. YANEZ[39], G. YODH[24], S. YOSHIDA[15], P. ZARZHITSKY[2], M. ZOLL[34]

32ND INTERNATIONAL COSMIC RAY CONFERENCE, BEIJING 2011

The IceTop Air Shower Array: detector overview, physics goals and first results

THE ICECUBE COLLABORATION[1]
[1]*See special section in these proceedings*

Abstract: IceTop, the surface component of the IceCube Neutrino Observatory at the South Pole, is an air shower array with an area of 1 km^2. The detector is primarily designed to study the mass composition of primary cosmic rays in the energy range from about 10^{14} eV to 10^{18} eV by exploiting the correlation between the shower energy measured in IceTop and the energy deposited by muons in the deep ice. Construction of IceCube, including the IceTop component, was completed in December 2010. The final detector configuration, first operation and performance experiences, the development of an analysis framework, and first results will be reported.

Corresponding author: Hermann Kolanoski (*Hermann.Kolanoski@desy.de*)
Institut für Physik, Humboldt-Universität zu Berlin, D-12489 Berlin, Germany

Keywords: Cosmic rays, IceCube, IceTop

1 Introduction

The Neutrino Observatory IceCube is a 1-km^3 detector situated in the ice of the geographic South Pole at a depth of about 2000 m. IceTop, the surface component of IceCube, is an air shower array covering an area of 1 km^2. The prime purpose of IceTop is the determination of the mass composition of primary cosmic rays in the energy range from about 10^{14} eV to 10^{18} eV. In the 'knee' region, at several PeV, the spectral index of the observed cosmic ray energy spectrum changes. Several experiments found this change to be accompanied by a change in the chemical composition of the primaries. However, details of the features are not well known. In particular, there may be at the high end of the IceTop energy range another change of the spectral index and an accompanying change of the composition, possibly indicating the transition from galactic to extra-galactic origin of cosmic rays. An improvement of the experimental situation in this energy range – between direct measurements with balloons and satellites and the highest energies tackled by experiments like HiRes and Auger – is one of the main goals of cosmic ray physics with IceCube.

The mass determination from extended air showers (EAS) is notoriously difficult because the measurements are indirect and have to rely on models for the hadronisation processes. Observables sensitive to the primary mass composition are mainly the height of the shower maximum (measured through fluorescence, Cherenkov or radio emission) and the number of muons in a shower. Concerning the muon rate, the highest energy muons stemming from the first interactions in the higher atmosphere are most closely correlated to the mass of the primary nucleus. IceCube, in combination with IceTop, offers the unique possibility to observe these muons, typically with initial energies above about 500 GeV, in the deep ice in coincidence with the mostly electromagnetically deposited shower energy measured at the surface. This provides an exceptionally powerful method for the determination of the mass composition.

To scrutinize the dependence on hadronisation models, several alternative methods for studying mass composition have been developed by the IceCube collaboration. Other mass sensitive observables are for example: the shower absorption in the atmosphere at different zenith angles, the number of dominantly low-energy muons in the surface detector, and other shower properties such as shower age and shower front curvature.

The IceTop array has additionally been used to study high-p_T muons, PeV-gammas and transient events, such as the radiation effects of solar flares. It also serves as a veto for the detection of downward-going neutrinos with IceCube and for direction calibration.

2 The detector

The IceCube construction was completed in December 2010. The results presented here are based on data taken with smaller detector configurations.

IceCube: The main component of Icecube is an array of 86 strings equipped with 5160 light detectors in a volume

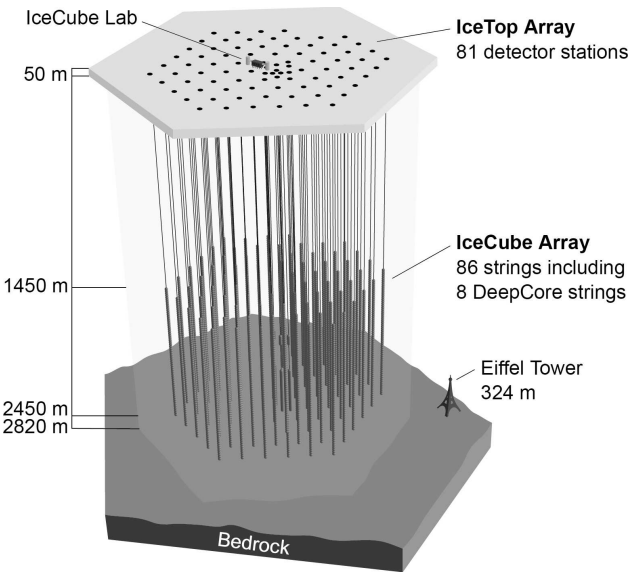

Figure 1: The IceCube Observatory with its components DeepCore and IceTop.

of 1 km^3 at a depth between 1450 m and 2450 m (Fig. 1). In the lower part of the detector a section called DeepCore is more densely instrumented. The main purpose of IceCube is the detection of high energy neutrinos from astrophysical sources via the Cherenkov light of charged particles generated in neutrino interactions in the ice or the rock below the ice.

IceTop: The IceTop air shower array is located above IceCube at a height of 2832 m above sea level, corresponding to an atmospheric depth of about 680 g/cm^2. It consists of 162 ice Cherenkov tanks, placed at 81 stations and distributed over an area of 1 km^2 on a grid with mean spacing of 125 m (Fig. 1). In the center of the array, three stations have been installed at intermediate positions. Together with the neighbouring stations they form an in-fill array for denser shower sampling. Each station comprises two cylindrical tanks, 10 m apart from each other, with a diameter of $1.86\,\mathrm{m}$ and filled with $90\,\mathrm{cm}$ ice. The tanks are embedded into the snow so that their top surface is level with the surrounding snow to minimize temperature variations and snow accumulation caused by wind drift. However, snow accumulation (mainly due to irregular snow surfaces) cannot be completely avoided so that the snow height has to be monitored (see ref. [1]) and taken into account in simulation and reconstruction (currently this is still a source of non-negligible systematic uncertainties).

Each tank is equipped with two 'Digital Optical Modules' (DOMs), each containing a $10''$ photo multiplier tube (PMT) to record the Cherenkov light of charged particles that penetrate the tank. In addition, a DOM houses complex electronic circuitry supplying signal digitisation, readout, triggering, calibration, data transfer and various control functions. The most important feature of the DOM electronics is the recording of the analog waveforms in $3.3\,\mathrm{ns}$ wide bins for a duration of $422\,\mathrm{ns}$. DOMs, electronics and readout scheme are the same as for the in-ice detector.

Figure 2: Reconstruction of shower parameters from the lateral distribution.

The two DOMs in each tank are operated at different PMT gains ($1 \cdot 10^5$ and $5 \cdot 10^6$) to cover a dynamic range of more than 10^4. The measured charges are expressed in units of 'vertical equivalent muons' (VEM) determined by calibrating each DOM with muons (see ref. [1]).

To initiate the readout of DOMs, a local coincidence of the two high gain DOMs of a station is required. This results in a station trigger rate of about 30 Hz compared to about 1600 Hz of a single high gain DOM at a threshold of about 0.1 VEM. The data are written to a permanent storage medium, and are thus available for analysis, if the readouts of six or more DOMs are launched by a local coincidence. This leads to a trigger threshold of about 300 TeV. Additionally, IceTop is always read out in case of a trigger issued by another detector component (and vice versa). For each single tank above threshold, even without a local coincidence, condensed data containing integrated charge and time stamp are transmitted. These so-called SLC hits (SLC = 'soft local coincidence') are useful for detecting single muons in showers where the electromagnetic component has been absorbed (low energies, outer region of showers, inclined showers).

For monitoring transient events via rate variations, the time of single hits in different tanks with various thresholds are histogrammed.

3 Shower reconstruction

For each triggered tank in an event, time and charge of the signal are evaluated for further processing. Likelihood maximisation methods are used to reconstruct location, direction and size of the recorded showers. In general, signal times contain the direction information, and the charge distribution is connected to shower size and core location. The standard analysis requires five or more triggered stations leading to a reconstruction threshold of about $500\,\mathrm{TeV}$. A constant efficiency is reached at about $1\,\mathrm{PeV}$, depending on shower inclination. For small showers an effort was launched to decrease the threshold to about $100\,\mathrm{TeV}$ with a modified reconstruction requiring only three stations.

The lateral signal distribution is fitted by a function which describes the logarithm of the tank signals as a second order polynomial in the logarithm of the distance from the shower axis (Fig. 2). Characterizing the shower size the signal S_{125} at a reference radius $R_{\rm ref} = 125\,{\rm m}$, coinciding with the grid spacing, has been used for the analyses presented in this paper. Studies of alternative lateral distribution functions are reported in a separate contribution to this conference [2].

The true energy spectrum is obtained by unfolding the S_{125} distribution in different zenith angular ranges. Since the unfolding matrices depend on the primary mass composition, a mass model has to be assumed [3] or the correlation with mass sensitive observables, most notably the muon number in the deep detector, has to be exploited for an essentially two-dimensional unfolding [4].

The energy resolution improves with energy and approaches 0.05 in $\log_{10} E$, or 12 % in E, at about 10 PeV for zenith angles less than 30°. The angular resolution is better than 1°, almost independent of energy and zenith angle. The detector coverage is $A\,\Omega \approx 3\,{\rm km}^2\,{\rm sr}$ for IceTop alone and $A\,\Omega \approx 0.3\,{\rm km}^2\,{\rm sr}$ for coincidences with the in-ice detector.

4 First results

Energy spectrum: The shower reconstruction from IceTop signals has been developed mainly using data taken with 26 stations (nearly 1/3 of the complete detector) in 2007. The spectra of the shower size parameter S_{125} for three different zenith angular ranges are shown in Fig. 3. Except for the threshold region, this parameter is a close proxy for the primary energy for a given zenith angle range. The relation between S_{125} and the true energy is mass dependent. Under the assumption of an isotropic cosmic ray flux, the S_{125} spectra for different zenith angles should yield the same energy spectrum. It has been shown that this can only be achieved under the assumption of a mixed composition [3].

A first evaluation of IceTop data from the 2010 season with 79 IceCube strings and 73 IceTop stations is reported elsewhere in these proceedings [5].

Mass composition using IceTop and deep-ice coincidences: As emphasized in the introduction, a strength of IceCube is the possibility to measure high energy muons in the deep ice in coincidence with the shower reconstructed in IceTop. The first analysis of such coincident data is presented at this conference [4]. The data set is constrained to a small fraction of the detector and a relatively short time period (about 1 month). However, the results are currently more affected by systematic uncertainties than by statistics.

Figure 4 shows a simulation of the correlation between the parameter K_{70}, which measures the muon energy in the deep ice, and the shower size parameter S_{125}, which is a measure of the electromagnetic component of the shower. Different primary masses populate different bands in this

Figure 3: Measured spectrum of the shower size parameter S_{125} for three different zenith angular ranges (data from 6 months with 26 IceTop stations).

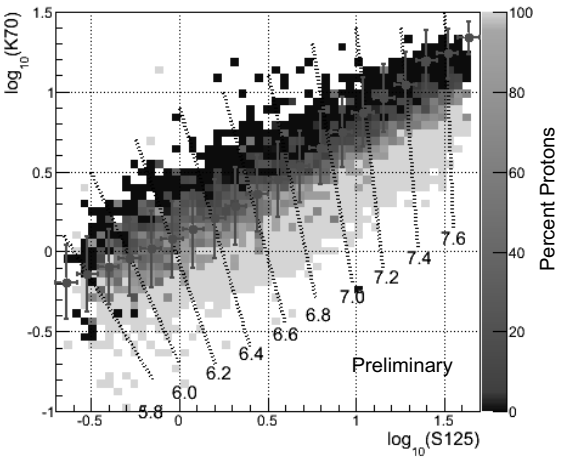

Figure 4: Mass composition measurement: plotted is the muon energy parameter K_{70} measured in the deep ice versus the shower size S_{125}. The band is obtained by simulating proton and iron primaries. The shading indicates the proton content, with 100% protons at the bottom und 100% iron at the top. Indicated are also curves of constant primary energy as determined by a neural net (the labels are in units $\log_{10} E/{\rm GeV}$). The points and the vertical bars are averages and dispersions, respectively, of the measured experimental distributions of a $\log_{10} S_{125}$ bin (indicated by the horizontal bars) projected unto the $\log_{10} K_{70}$ axis.

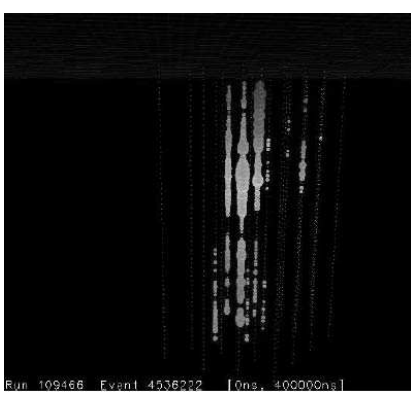

Figure 5: IceCube event display showing light signals in DOMs: Candidate muon bundle with a high-$p_{\rm T}$ muon (on the right).

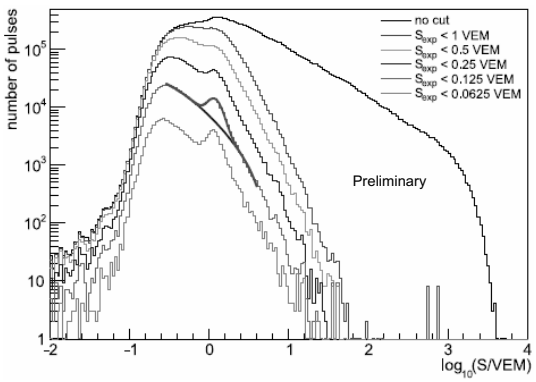

Figure 6: Muon counting in IceTop: Distribution of tank signals for various cuts on the signal expectation S_{exp} in the energy range between 1 and 30 PeV.

plot. Indicated are also curves of constant primary energy. The data points in $\log S_{125}$ bins are plotted with the dispersion of their distribution along the K_{70} axis.

With a neural network, the primary energy and a parameter related to $\ln A$ (A is the atomic mass number) has been determined yielding an energy and average $\ln A$ spectrum between 1 and 50 PeV. The method allows for the extraction of multiple mass contributions from fits to the neural network output, see details in ref. [4].

High-p_T muons: Prompt decays of heavy flavour hadrons occurring in the first interactions are expected to produce muons with large transverse momentum. The predictions are still very model dependent. In these proceedings, an analysis is presented [6] where high-p_T muons have been found as single tracks separated from a muon bundle by more than 200 m (Fig. 5). Current work concentrates on understanding the systematic uncertainties in the resulting p_T distribution.

Searching for PeV gamma rays: IceCube can efficiently distinguish PeV gamma rays from the background of cosmic rays by exploiting coincident in-ice signals as veto. Gamma-ray air showers have a much lower muon content than cosmic ray air showers of the same energy. Candidate events are selected from those showers that lack a signal from a muon bundle in the deep ice. Results of one year of data, taken in the 2008/2009 season when the detector consisted of 40 strings and 40 surface stations, are presented at this conference [7]. The projected gamma-ray sensitivity of the final detector is also given.

Muon counting in IceTop: The muon content of a shower is a mass sensitive observable since heavier primaries tend to have a higher muon abundance. Although the number of high energy muons in the muon bundle near the shower core is most sensitive, muons counted at the surface (at typically much lower energies than in the deep ice) provide additional information on the mass. The comparison of both methods allows one to test hadronisation models.

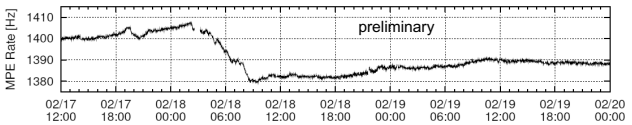

Figure 7: Average scaler rates of several tanks in IceTop during a period in February 2011 when a Forbush decrease occured.

Muonic and electromagnetic signals in IceTop can in general not be distinguished. However, muons show up as a relatively constant signal of about 1 VEM at larger distances from the shower axis where the expectation value of a tank signal, S_{exp}, becomes small compared to a muon signal (S_{exp} is obtained from the fit to the lateral shower distribution). As shown in Fig. 6, the muon signal becomes more and more prominent when requiring smaller S_{exp}. For $S_{exp} < 0.125$ VEM the figure illustrates that the number of muons can be well fitted. Comparing these muon numbers as a function of energy to simulations of different primary masses an independent information on the mass composition is obtained.

Heliospheric physics: The IceTop tanks detect secondary particles produced by cosmic rays in the multi-GeV energy regime interacting in the atmosphere with a counting rate exceeding 1 kHz per detector. With IceTop, heliosperic disturbances of this rate can be studied with very good time resolution. Since each detector has a different threshold setting, it is also possible to estimate the energy spectrum of the cosmic rays related to such events. In an IceCube contribution to this conference [8] the performance during a Forbush decrease observed in February 2011 is demonstrated (Fig. 7).

Other cosmic ray results: At this conference the Icecube Collaboration also reports results on the observation of cosmic ray anisotropies in the southern sky [9]. These results and the cosmic ray studies in ref. [10] use all muons detected in the deep detector which gives a much larger angular coverage.

References

[1] IceCube Collaboration, paper 899, these proceedings.
[2] IceCube Collaboration, paper 379, these proceedings.
[3] F. Kislat for the IceCube Coll., Astrophys. Space Sci. Trans. 7 (2011) 175.
[4] IceCube Collaboration, paper 923, these proceedings.
[5] IceCube Collaboration, paper 838, these proceedings.
[6] IceCube Collaboration, paper 323, these proceedings.
[7] IceCube Collaboration, paper 939, these proceedings.
[8] IceCube Collaboration, paper 735, these proceedings.
[9] IceCube Collaboration, papers 305, 306, 308, these proceedings.
[10] IceCube Collaboration, papers 85, 662, these proceedings.

32ND INTERNATIONAL COSMIC RAY CONFERENCE, BEIJING 2011

Cosmic Ray Composition from the 40-string IceCube/IceTop Detectors

THE ICECUBE COLLABORATION[1]
[1]*See special section in these proceedings*

Abstract: The IceCube Observatory at the South Pole is composed of a deep detector and a surface detector, IceTop, both of which use Cherenkov light to detect charged particles. Cosmic ray air showers contain multiple particle components: in particular, electrons and muons detectable at the surface by IceTop, and high-energy muons detectable by the deep IceCube detector, in relative amounts that depend on the primary cosmic ray mass. Thus, coincident events can be used to measure both the energy and the mass composition. Here, a neural network is trained with simulations to map observables from the two detectors (input) into energy and mass estimators (output). Experimental data is then run through the same network, to measure the energy spectrum and average logarithmic mass of cosmic rays in the energy range of about 1-30 PeV.

Corresponding authors: K. Andeen[2] (*karen.andeen@icecube.wisc.edu*), K. Rawlins[3], T. Feusels[4]
[2]*Dept. of Physics, University of Wisconsin-Madison, WI 53706, USA (now at Rutgers University)*
[3]*Dept. of Physics and Astronomy, University of Alaska Anchorage, AK 99508, USA*
[4]*Dept. of Physics and Astronomy, Gent University, B-9000 Gent, Belgium*

Keywords: mass; composition; knee; IceCube; IceTop

1 Introduction

Measuring more than one particle component of a cosmic ray air shower is a powerful tool for separating light and heavy nuclei in Extensive Air Shower (EAS) data, at energies at the knee and above where direct measurements of cosmic rays are not possible. The IceCube Observatory at the South Pole is being used in such a manner, with an array of light sensors (Digital Optical Modules, or DOMs) buried on strings between 1450 and 2450 m (herein "IceCube") together in coincidence with a corresponding array of DOMs in frozen water tanks on the surface ("IceTop"). An IceTop "station" is two tanks separated by 10 m; IceCube strings and IceTop stations are separated by 125 m [1].

Both instruments measure the Cherenkov light emitted by charged particles through the surrounding medium. In IceTop, the medium is water frozen in tanks at the site. The DOMs in the tanks measure light from the electromagnetic and GeV muonic components of the EAS. In IceCube, the medium is the Antarctic icecap, and the deeply-buried DOMs measure light from high-energy (TeV) muons bundled near the central axis of the shower.

2 Reconstruction

Events in IceTop are reconstructed by a likelihood method [3], comparing the detected signal locations, charges, and times from hit stations (as well as the locations of not-hit stations) to what is expected from a cosmic ray EAS. Signal *times* are compared to an expected timing profile, and signal *charges* are compared to an expected lateral distribution function (LDF). The LDF used, a function of the perpendicular distance from the shower axis, r, is known as the "Double Logarithmic Parabola,":

$$S(r) = S_{\rm ref} \cdot \left(\frac{r}{R_{\rm ref}}\right)^{-\beta-\kappa\log_{10}\left(\frac{r}{R_{\rm ref}}\right)} . \qquad (1)$$

The logarithm of the signals S are assumed to have normal distributions, and are expressed in units of "vertical equivalent muons" (VEM). Here, $R_{\rm ref}$ represents a "reference distance" from the shower axis, and $S_{\rm ref}$ is the signal strength at that reference distance. The reference distance found to have the most robust measurement at these energies is 125 m [3], so S_{125} is the observable representing the "shower size".

Events in IceCube are reconstructed with a similar philosophy: the signals N_{PE}, measured in photoelectrons, are compared to an LDF which is a function of perpendicular

32ND INTERNATIONAL COSMIC RAY CONFERENCE, BEIJING 2011

Seasonal Variations of High Energy Cosmic Ray Muons Observed by the IceCube Observatory as a Probe of Kaon/Pion Ratio

THE ICECUBE COLLABORATION[1]
[1]*See special section in these proceedings*

Abstract: The high statistics of cosmic ray induced muon events detected by the IceCube Observatory makes it possible to study the correlation of muon intensity with the stratospheric temperature over Antarctica with high precision. Using 150 billion events collected by IceCube experiment over 4 years, the muon rate was found to be highly correlated with daily variations of the stratospheric temperature and exhibits a $\pm$ 8% annual modulation. The correlation between the muon rate and the upper atmospheric temperature is related to the relative contribution of π and K to the production of muons. Therefore it is possible to estimate the K/π ratio from the seasonal variation of the muon rate, which was found to be 0.09 ± 0.04 at cosmic ray median energy of about 20 TeV.

Corresponding authors: P. Desiati[1], T. Kuwabara[2], T.K. Gaisser[2], S. Tilav[2], D. Rocco[1]
[1]*IceCube Research Center and Dept. of Physics, University of Wisconsin, Madison, WI 53706, U.S.A.*
[2]*Bartol Research Institute and Dept. of Physics and Astronomy, University of Delaware, Newark, DE 19716, U.S.A.*

Keywords: cosmic muons, seasonal modulation, IceCube

1 Introduction

When cosmic ray particles enter the Earth's atmosphere, they generate a hadronic cascade in which mesons are produced, primarily pions and kaons. These mesons can either interact again or decay into muons. The relative probability of decay or interaction depends on the local density of the atmosphere, which in turn depends on the temperature [1]. The differential flux of muons with energies larger than 100 GeV can be described with good approximation as [2]

$$\phi_\mu(E_\mu,\theta) = \phi_N(E_\mu) \times \left\{ \frac{A_{\pi\mu}}{1 + B_{\pi\mu}\cos\theta^\star\, E_\mu/\epsilon_\pi} + \frac{A_{K\mu}}{1 + B_{K\mu}\cos\theta^\star\, E_\mu/\epsilon_K} \right\}, \quad (1)$$

where $\phi_N(E_\mu)$ is the primary spectrum of nucleons (N) evaluated at the energy of the muon. The first term in Eq. 1 corresponds to muon production from leptonic and semileptonic decays of pions, while the second term is related to kaons. The constants $A_{\pi\mu}$ and $A_{K\mu}$ include the branching ratio for meson decay into muons, the spectrum weighted moments of the cross section for a nucleon to produce secondary mesons, and those of the meson decay distribution. The denominators in Eq. 1 reflects the competition between decay and interaction of secondary mesons in the atmosphere. When $E_{\pi,K} < \epsilon_{\pi,K}/\cos\theta^\star$, the meson decay is the dominant process, and muons are produced with the same spectral index as the parent cosmic rays. At high energy meson interaction dominates and the corresponding muon spectrum becomes one power steeper than the primary spectrum. The characteristic critical energies $\epsilon_{\pi,K}$ at a given atmospheric depth are inversely proportional to the atmosphere's density at that point, and therefore are affected by temperature variations. In an isothermal approximation of the atmosphere, the density is described by an exponential with a scale height of $h_\circ \approx 6.19$ km (over Antarctica). The numerical value applies to the lower stratosphere, where most of the muons are generated. In this approximation $\epsilon_{\pi,K}$ are proportional to the atmosphere's temperature in the perfect gas state limit. At a mean atmospheric temperature of $T_\circ = 211°$K the critical energies are $\epsilon_\pi = 111$ GeV and $\epsilon_K = 823$ GeV. The dependence of the critical energies on temperature is the main source of the seasonal variation in muon rate. This modulation was studied by underground experiments such as MACRO [3], LVD [4] and MINOS [5], and by AMANDA [6] and IceCube [7]. Here we update the analysis with four years of IceCube data with an emphasis on the systematic effects that can be studied with a very large amount of data.

2 Temperature Correlation

The relation between the variation of temperature and the variation of muon intensity at a particular energy and zenith angle can be expressed in terms of a theoretical correlation

coefficient calculated from Eq. 1 as

$$\alpha_\mu(E_\mu,\theta) = \frac{T}{\phi_\mu(E_\mu,\theta)}\frac{\partial\phi_\mu(E_\mu,\theta)}{\partial T}, \qquad (2)$$

which depends explicitly on the characteristic critical energies $\epsilon_{\pi,K}$.

Measured rates depend on the convolution of the muon differential spectrum with the detector response, which depends on muon energy and zenith angle. To compare with measurements, it is therefore necessary to calculate a weighted correlation coefficient as

$$\alpha_T^{th}(\theta) = \frac{T\cdot\frac{\partial}{\partial T}\int dE_\mu\,\phi_\mu(E_\mu,\theta)\,A_{eff}(E_\mu,\theta)}{\int dE_\mu\,\phi_\mu(E_\mu,\theta)\,A_{eff}(E_\mu,\theta)}, \qquad (3)$$

where $A_{eff}(E_\mu,\theta)$ is the effective detector area obtained from simulation. Eq. 3 defines the correlation coefficient for a particular zenith angle θ. The total correlation coefficient is then obtained by averaging $\alpha_T^{th}(\theta)$ over θ with a weight given by the observed event angular distribution. With this definition the variation in muon intensity I_μ is given by

$$\frac{\Delta I_\mu}{I_\mu} = \alpha_T^{th}\,\frac{\Delta T_{eff}}{T_{eff}}, \qquad (4)$$

where T_{eff} is the effective atmospheric temperature as defined below. Since the rate R_μ of observed muons is proportional to the incident muon intensity I_μ, it is correlated with the effective temperature as well

$$\frac{\Delta R_\mu}{\langle R_\mu\rangle} = \alpha_T^{exp}\,\frac{\Delta T_{eff}}{\langle T_{eff}\rangle}, \qquad (5)$$

where α_T^{exp} is the experimentally determined correlation coefficient.

Since muon production occurs over an extended portion of the upper atmosphere and the temperature depends on altitude, it is necessary to define a parameter referred to as effective temperature, in order to quantify the relationship between variations in temperature and those in measured muon rate.

The pion and kaon terms in Eq. 1 are derived from the integral over the atmospheric slant depth X (in g/cm^2) of the muon production spectrum $P_\mu(E_\mu,\theta,X)$, which in turn is given by the probability distribution for meson decay to muons integrated over the parent meson spectrum [2].

The effective temperature as a function of muon energy and zenith angle is defined as the actual temperature profile weighted by the muon production spectrum

$$T_{eff}(E_\mu,\theta) = \frac{\int dX\,P_\mu(E_\mu,\theta,X)T(X)}{\int dX\,P_\mu(E_\mu,\theta,X)}, \qquad (6)$$

where $P_\mu(E_\mu,\theta,X)$ is the sum of muon production spectrum from pion and kaon contributions. The rationale for this definition is that the depth dependence of the muon production spectrum weights the temperature with the regions of the atmosphere where the meson decay to muons occurs. The critical energies that appear in the production spectrum are evaluated at the mean temperature, $T_\circ$, but the production profile does not depend strongly on temperature.

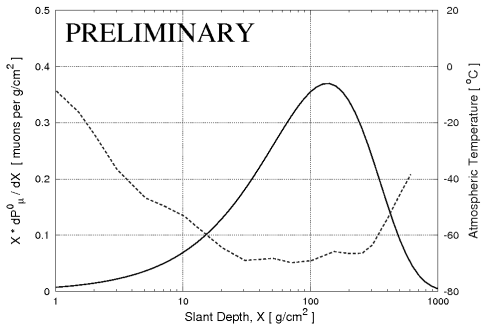

Figure 1: The differential weighting function used in the calculation of the T_{eff}, as a function of atmospheric depth X (continuous line), superimposed on the average atmospheric temperature profile (dashed line).

This formulation of the effective temperature differs from that in Grashorn et al. [8], where the low energy limit of the temperature derivative of muon production spectrum produces an unphysical discontinuity. The IceCube observatory is located at a depth of >1.3 km.w.e./cosθ so only muons with energies above about 400 GeV/cosθ can reach and trigger the detector. At these energies muon decay and energy loss in the atmosphere are negligible. This enables us to use analytic forms for muon production analogous to Eq. 1 without accounting for decay and energy loss of muons in the atmosphere and hence to obtain a physically correct result without any discontinuity.

To compare predictions with measurements it is necessary to determine the convolution with the detector response function

$$T_{eff}(\theta) = \frac{\int E_\mu\,\int dX\,P_\mu(E_\mu,\theta,X)\,A_{eff}(E_\mu,\theta)\,T(X)}{\int E_\mu\,\int dX\,P_\mu(E_\mu,\theta,X)\,A_{eff}(E_\mu,\theta)}, \qquad (7)$$

where the denominator, as in Eq. 3, is the total measured muon intensity. As for the correlation coefficient, the total effective temperature T_{eff} is the weighted average of Eq. 7 over the event zenith distribution. Fig. 1 shows the differential weighting function used in the calculation of the effective temperature along with the average atmospheric temperature profile over the seasons. It peaks at about 100 g/cm^2, which is where most of the muons are produced.

3 Muon and Temperature Data

In this analysis we used 150 billion muon events collected by the partially completed IceCube Observatory from March 2007 to April 2011 (see [9] for an overview on IceCube). These events are generated by cosmic rays with median energy of about 20 TeV.

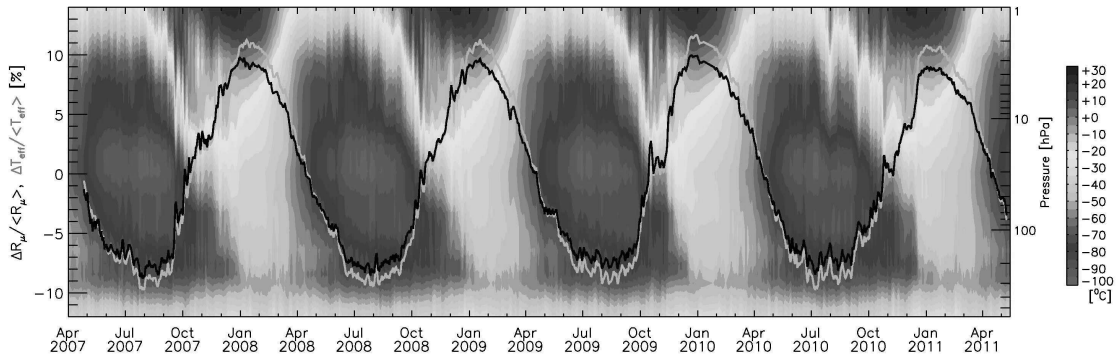

Figure 2: The daily atmospheric temperature profiles over Antarctica produced by NASA AIRS instrument on board the Aqua satellite [10] are shown from 2007 to 2011 (in color code), along with the relative modulation in the measured muon event rate (black line) and the relative variation of the effective temperature (grey line). Note that the statistical uncertainties in the data are between about 0.1 Hz (in 2007) and about 0.16 Hz (in 2011) on the daily rates. The corresponding uncertainties on the relative rate variations are 0.02 % and 0.008 %, respectively.

The muon rate increased substantially over these four years as new detectors were added during each construction season. As the instrumented volume increased, the probability that one data record included two or more separate cosmic-ray events increased from about 1% to about 4%. A correction to the daily recorded rate was therefore applied to obtain a corrected rate of muon events, R_μ.

The atmospheric temperature profile data used in this analysis were collected by the NASA Atmospheric Infrared Sounder (AIRS) on board the Aqua satellite. Daily atmospheric temperatures at 20 different pressure levels from 1 to 600hPa above the South Pole were obtained from the AIRS Level 3 Daily Gridded Product available on NASA Goddard Earth Sciences, Data and Information Services Center (GES DISC) [10]. Using these data the daily effective temperature T_{eff} was calculated based on the zenith-weighted average of Eq. 7.

4 Results and Determination of K/π Ratio

Fig. 2 shows the measured $\frac{\Delta R_\mu}{\langle R_\mu \rangle}$ as a black continuous line along with $\frac{\Delta T_{eff}}{\langle T_{eff} \rangle}$ as a black dashed line. The figure also shows the actual atmospheric temperature profile as a function of pressure level (equivalent to atmospheric depth X). The statistical uncertainties in the measured muon rate are too small to show in the figure. Note that besides the large seasonal modulation, the daily muon rate is strongly correlated with short time temperature variations in the upper atmosphere.

Based on Eq. 5, the experimental temperature coefficient was determined from regression analysis and found to be $\alpha_T^{exp} = 0.860 \pm 0.002$ (stat.) $\pm$ 0.010 (syst.). The experimental systematic uncertainty on α_T^{exp} is dominated by the effective area $A_{eff}(E_\mu, \theta)$, which is used in the calculation of the effective temperature and of the theoretical correlation coefficient in Eq. 3. Most of the detected muons range out within the large instrumented volume of IceCube, and the energy profile of the effective area depends on the distribution of depths the muons reach within the array. The spread on this distribution, translates into an estimated uncertainty in the experimental correlation coefficient of 0.01.

Since the temperature correlation coefficient depends on the relative contribution of pions and kaons, it is possible to use the seasonal variations of the muon rate to determine the K/π ratio.

The effective temperature T_{eff} is relatively insensitive to variations in the cosmic ray spectral index, the proton attenuation length, the critical energies and K/π ratio because the dependence cancels to a large extent due to the normalization in Eq. 7.

The theoretical correlation coefficient α_T^{th}, on the other hand, depends primarily on the critical energies and on the K/π ratio. Changing the cosmic ray spectral index and proton attenuation length within a wide range, has an effect smaller than 1%. Therefore it is possible to use the parameters for attenuation lengths and spectrum weighted moments from Ref. [2], assuming a cosmic ray spectral index of -2.7. The critical energies evaluated at the average effective temperature of $T_\circ = 211°$K are used.

In particular, the kaon to pion ratio $R_{K/\pi} = \frac{Z_{NK}}{Z_{N\pi}}$ depends on the spectrum weighted moments Z_{NK} and $Z_{N\pi}$ of the cross section for a nucleon N to produce secondary kaons and pions, respectively, from a target nucleus in the atmosphere. The dependence on the spectrum weighted moments Z_{NK} and $Z_{N\pi}$ is implicit in the parameters $A_{\pi\mu}$ and $A_{K\mu}$ in Eqs. 1, 3, 7.

The nominal value of K/π ratio is taken to be [2]

$$R_{K/\pi} = \frac{0.0118}{0.079} = 0.149 \pm 0.060, \qquad (8)$$

which is based on laboratory measurements below 100 GeV center of mass energy. The 40% uncertainty corresponds to that in the current cosmic ray interaction models [11].

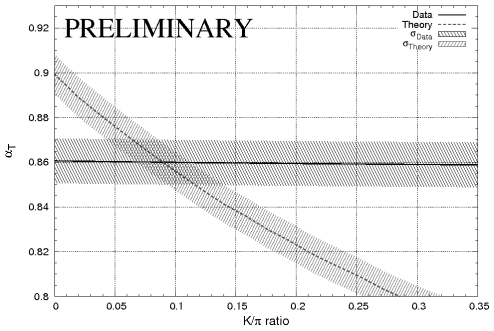

Figure 3: The preliminary α_T^{exp} determined by IceCube as a function of the K/π ratio (continuous line), with its error given by the band, and the predicted α_T^{th} (dashed line) with the corresponding error given by the band. The intersection region between the two bands is at $R_{K/\pi} = 0.09 \pm 0.04$.

By calculating the theoretical correlation coefficient α_T^{th} as a function of $R_{K/\pi}$ and comparing it with the experimental value, it is possible to measure the kaon to pion ratio for proton interaction with atmospheric nuclei (mainly nitrogen) at cosmic ray particle energy of 20 TeV.

Fig. 3 shows the experimental and theoretical values of α_T as a function of K/π ratio for the IceCube data. While, as mentioned above, α_T^{exp} is almost insensitive to $R_{K/\pi}$, the value of α_T^{th} has a strong dependence. Since the statistical uncertainties are very small, the band on α_T^{exp} is dominated by systematic uncertainties. The band on α_T^{th} reflects the theoretical uncertainties in the calculation of the correlation coefficient mentioned above, and conservatively estimated to be 1%. The crossover in Fig. 3 is at $R_{K/\pi} = 0.09 \pm 0.04$. Fig. 4 shows a comparison of the IceCube measurement with other observations.

5 Conclusions

Using 150 billion cosmic ray induced muon events collected in four years by IceCube, a strong correlation of the daily observed muon rate with the stratospheric temperature was observed, along with a $\pm 8\%$ annual modulation. The K/π ratio at 20 TeV cosmic ray energies was determined by comparing the observed temperature correlation coefficient with the theoretical one, and found to be $R_{K/\pi} = 0.09 \pm 0.04$.

The value obtained with IceCube implies that $Z_{NK} \sim 0.0071$, which is about 40% lower than its nominal value from Ref. [2]. In calculating the theoretical correlation coefficient the sum $Z_{NK} + Z_{N\pi}$ was kept constant to its nominal value 0.0908. One way to reconcile the measurement of $R_{K/\pi}$ with other results is by reducing the amount of associated production $pN \to nK^+$. Keeping the nominal value of $Z_{NK^-} = 0.0028$, while reducing Z_{pK^+} from its nominal value of 0.0090 to 0.0043 is also likely to give a better agreement with recent measurements of the ratio of

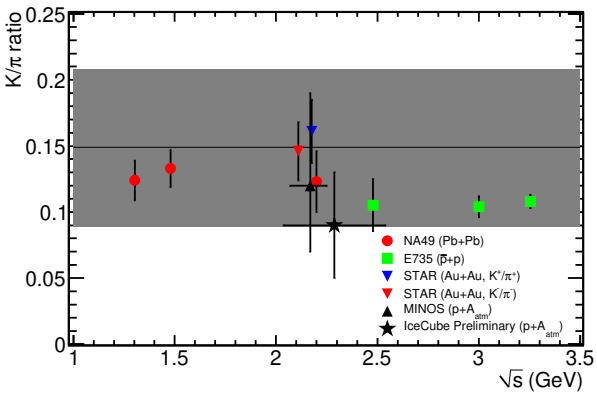

Figure 4: A compilation of selected measurements of K/π for various center of mass energies. Data points are from NA49 [12, 13], E735 [14], STAR [15] and MINOS [5]. The horizontal line and gray band represents the reference value K/π ratio 0.149 ± 0.060 [2, 11].

the atmospheric muon charge ratio from MINOS [16] and OPERA [17].

6 Acknowledgements

The temperature data used in this study were acquired as part of the NASA's Earth-Sun System Division and archived and distributed by the Goddard Earth Sciences (GES) Data and Information Services Center (DISC) Distributed Active Archive Center (DAAC).

References

[1] P.H. Barret, *et al.*, Rev. Mod. Phys., 1952, **24**(3), 133.
[2] T.K. Gaisser, 1990, Cosmic Rays and Particle Physics, ed. CUP
[3] M. Ambrosio, *et al.*, Astrop. Phys., 1997, **7**, 109.
[4] M. Selvi, Proc. of 31^{st} ICRC, 2009, Łòdż, Poland.
[5] P. Adamson, *et al.*, Phys.Rev., 2010, **D81**,01200.
[6] A. Bouchta, Proc. of 26^{th} ICRC, 1999, Salt Lake City, UT, U.S.A.
[7] S. Tilav, *et al.*, Proc. of 31^{st} ICRC, 2009, Łòdż, Poland, arXiv:1001.0776.
[8] E.W. Grashorn, *et al.*, Astrop. Phys., 2010, **33**, 140.
[9] H. Kolanoski, IceCube summary talk, these proceedings.
[10] http://disc.sci.gsfc.nasa.gov/AIRS/data-holdings.
[11] G.D. Barr, *et al.*, Phys. Rev., 2006, **D74**, 094009.
[12] S.V. Afanasiev, *et al.*, Phys. Rev., 2004, **C66**, 054902.
[13] C. Alt, *et al.*, Eur. Phys. J. C, 2006, **45**, 343.
[14] T. Alexopoulos, *et al.*, Phys. Rev., 1993, **D48**, 984.
[15] C. Adler, *et al.*, Phys .Lett., 2004, **B595**, 143.
[16] P. Adamson, *et al.*, Phys. Rev., 2007, **D76**, 052003.
[17] N. Agafonova, *et al.*, 2010, arXiv:1003.1907.

32ND INTERNATIONAL COSMIC RAY CONFERENCE, BEIJING 2011

Measurements of the Air Shower Parameters with IceTop

THE ICECUBE COLLABORATION[1]
[1]*See special sections in these proceedings*

Abstract: We study the lateral distribution function (LDF) of signals in the IceTop air shower detector as a function of distance from the air shower core. The completed IceTop detector consists of 81 stations with two tanks each. It can now study the signals at distances approaching 1 km from the core position. We discuss the general shape of lateral distributions of the signal and its dependence on the shower zenith angle and primary mass. We also show the simulated individual tank signal lateral distribution for a large number of simulated proton and iron showers. We find that the form of the lateral distribution function used for more widely spaced arrays of water Cherenkov detectors, Haverah Park and Auger in the EeV range, can also be used with appropriate parameters to describe IceTop data in the 10-100 PeV range.

Corresponding authors: Shahid Hussain[2] (*shahid@bartol.udel.edu*), Todor Stanev[2] (*stanev@bartol.udel.edu*), Serap Tilav[2] (*tilav@udel.edu*)
[2]*University of Delaware, Newark, DE 19716, U.S.A.*

Keywords: IceCube, IceTop, lateral distributions

1 Introduction

IceTop, the surface air shower array above the IceCube neutrino detector, was completed in the 2010/2011 deployment season. IceTop consists of 81 stations, each of which has 2 tanks of area 2.7 m^2 containing 90 cm of clear ice. The average distance between the tanks in a station is 10 m and the average distance between stations is 125 m. The Cherenkov light generated by the charged particles that hit the tanks is collected by two digital optical modules (DOMs) that run at different gains to increase the dynamic range. The signal strength is measured in vertical equivalent muon units (VEM), i.e. the signal that a 1 GeV vertical muon produces in the tank. A station triggers when there are signals above the threshold (0.16 VEM) in both tanks within one microsecond. In this way we avoid triggering on coincidental muons that belong to different atmospheric cascades.

The current shower reconstruction of IceTop events is based on a procedure which was designed when the array contained only 26 stations in a much smaller area [1]; the reconstruction procedure is applied to showers that trigger at least five stations. The signal lateral distribution function in this procedure does not include tanks with zero signal (i.e. tanks that do not trigger) and the fitting routine accounts for these tanks with a separate, no-hit probability, term in the likelihood function.

In this paper we instead use a lateral distribution function of the form [2]

$$S(r) \; = \; A \times r^{-(\eta + r/r_0)}, \qquad (1)$$

where $S(r)$ is the signal at a perpendicular distance r from the shower core in shower coordinates; η, r_0, and A are fit parameters. This form has been used for Haverah Park [3] and Auger [4] to fit showers observed with water Cherenkov tanks. IceTop is at a much higher altitude (2835 m) than HP (sea level) and significantly higher than Auger (1400 m) and collects data in a different primary energy range with detectors spaced by 125 m as compared to several hundred meters for HP and 1500 m for Auger. We investigate here the extent to which the lateral distribution form used for the other Cherenkov shower detectors scale to the location and energy range of IceTop. Everywhere in this paper, S(r) gives the signal strength at a perpendicular distance r from the shower core in shower coordinates. We include tanks with and without a signal directly in the lateral fit, both for simulated and observed air showers.

2 Monte Carlo Calculation

To study the lateral distribution we have simulated air showers initiated by protons and iron nuclei with fixed primary energies of 10 and 100 PeV and fixed zenith angles of 0, 25, and 45 degrees. Air showers are simulated with CORSIKA-SIBYLL [5] and the detector simulation uses Geant4 [6] for the tank response. 50 showers per primary

32ND INTERNATIONAL COSMIC RAY CONFERENCE, BEIJING 2011

Extensive Air Showers Measured by the 79-string IceCube Observatory at South Pole

THE ICECUBE COLLABORATION[1]
[1] *See special section in these proceedings*

Abstract: The IceCube Neutrino Observatory was completed in the 2010-11 Antarctic season with 86 deep strings and 81 surface stations. Between June 2010 and May 2011 IceCube collected high quality data with 73 stations and 79 strings. The performance of the detector as an air shower array to contribute to our understanding of the cosmic ray spectrum from the knee region up to 1 EeV will be demonstrated. The sensitivity to primary composition using high energy muon bundles seen by the IceCube array will also be discussed.

Corresponding authors: T. Feusels[2] (*tom.feusels@ugent.be*), S. Tilav[3] (*tilav@udel.edu*)
[2]*Dept. of Physics and Astronomy, University of Gent, B-9000 Gent, Belgium*
[3]*Bartol Research Institute and Dept. of Physics and Astronomy, University of Delaware, Newark, DE 19716, U.S.A.*

Keywords: IceTop; IceCube; Extensive Air showers; Muon bundles

1 Introduction

The IceCube Neutrino Observatory started taking data in May 2011 with the complete array of 81 surface stations and 86 strings in the deep Antarctic ice [1]. The array grid is shown in Figure 1. In the period of June 2010-May 2011, the surface air shower array, IceTop [2], was operated with 73 stations (146 ice Cherenkov tanks) positioned on a triangular grid with a 125 m spacing. The IceCube detector had 79 strings with 60 sensors on each string at depths between 1450 m and 2450 m in the ice. We refer to this configuration as IceTop-73/IceCube-79. The detector collected data with 98% uptime during this period.

IceCube, located at the geographic South Pole (altitude: 2835 m), is at an optimum atmospheric depth of 680 g/cm^2 where cosmic ray air showers in the PeV energy range are close to their shower maximum. In addition, with fast digital electronics for signal processing and high resolution waveforms, IceTop is in a unique position to make a detailed measurement of the cosmic ray energy spectrum in this energy region in a few years. About 30% of showers trigger both detectors; these are called coincident events. The energy deposited along the kilometer long tracks of the penetrating muon bundles in IceCube, when combined with the energy deposited on the surface in IceTop, provide a mass composition sensitive measurement.

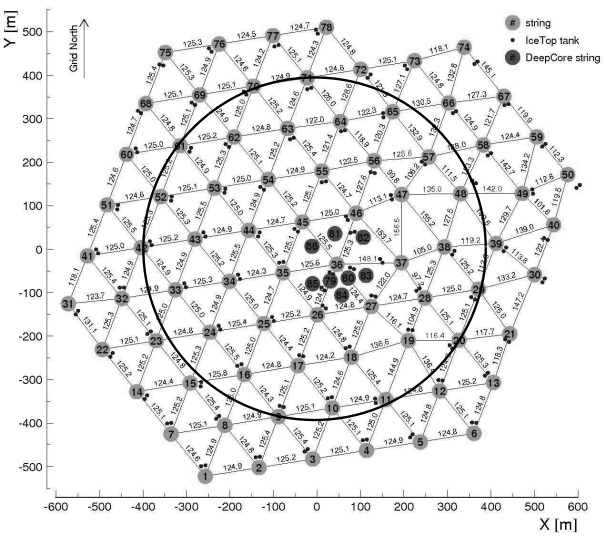

Figure 1: The surface map of IceCube in its completed configuration. IceTop Stations 1, 7, 14, 22, 31, 79, 80 and 81 were not yet deployed in 2010. The circle with a 400 m radius shows the containment criterium for the reconstructed shower core position.

In this paper we evaluate the performance of IceCube as a three dimensional Extensive Air Shower (EAS) array based on nine months of data from June 15, 2010 to March 15, 2011. The data is split into an austral winter dataset (Jun 15, 2010 - Nov 1, 2010) and an austral summer dataset

32ND INTERNATIONAL COSMIC RAY CONFERENCE, BEIJING 2011

Simulation of IceTop VEM calibration and the dependency on the snow layer

THE ICECUBE COLLABORATION[1]
[1]*See special section in these proceedings*

Abstract: Seven years of construction on the IceTop air shower array have culminated in the final detector setup of 162 ice-filled tanks. The tanks are paired as stations over an area of one square kilometer. A continuous and automatic procedure calibrates each tank via the extraction of the vertical equivalent muon peak in the tank charge spectrum. Over the years snow has drifted unevenly on top of the tanks. The overburden of snow influences the charge spectrum as the electromagnetic part of an air shower is attenuated more than the muonic part. The impact on individual tanks affects trigger rates and the air shower event structure. We will present tank response studies with Monte Carlo simulations and compare them to measured IceTop charge spectra in light of the varying thickness of the snow layer.

Corresponding authors: Arne Van Overloop[2] (*arne.vanoverloop@ugent.be*)
[2]*Department of Physics and Astronomy, University of Gent, B-9000 Gent, Belgium*

Keywords: Vertical Equivalent Muon; Calibration; Cosmic Rays; IceTop; Simulations

1 Introduction

IceTop is the cosmic ray surface detector of the IceCube Neutrino Observatory [1], which is located at the South Pole and was completed in March 2011. The final setup consists of 162 tanks paired in 81 stations on a hexagonal grid with horizontal separations of about 125 m. The array covers an area of one square kilometer at an altitude of 2835 m above sea level, which is equivalent to an average atmospheric depth of 680 g/cm^2. The location together with the geometry and the applied trigger settings make the array sensitive to cosmic rays with energies between 100 TeV and 1 EeV.

An IceTop tank acts as a calorimeter, converting energy deposited by charged relativistic particles into Cherenkov light. The reconstruction of air shower observables such as space angle (zenith and azimuth), core location (x and y) and shower size relies on a good understanding of the light signals in the individual IceTop tanks. A natural way to calibrate and simulate tanks with their individual responses is to use the reference signal - vertical equivalent muon (VEM) - that high energy vertical muons imprint in the charge spectra of each tank.

A schematic of an IceTop tank is shown in Figure 1. The tank is a cylindrical polyethylene vessel 186 cm in diameter and 130 cm in height covered with insulation. The walls are 6 mm thick and the inner part is covered with 4 mm thick diffusely reflective liner of Zirconium[1] fused polyethylene. Each tank is initially filled up to a height of about 90 cm with purified water. Afterwards the water freezes via a controlled top-to-bottom procedure that lasts for about 40 to 50 days. To minimize impurities or contamination and cracks in the ice during the freezing process, a degasser system in combination with a circulation pump extracts air, swirls the water slowly around and removes excess water. At the top of the ice volume, two Digital Optical Modules (DOMs) are mounted to record the Cherenkov light pattern created by through-going and stopping particles. A DOM [2] is an ensemble of a photomultiplier tube (PMT) and digitising, communication and operation electronics inside a glass pressure sphere. In data taking mode the two PMTs inside one tank operate at a different voltage setting, enlarging the dynamic range in linear pulse charge assignment. Moreover, in case one DOM in a tank fails, the tank is not lost in further physics analysis. The ice surface and the two DOMs are covered with perlite, a volcanic ash, that acts as an insulator and prevents light from entering the ice volume and triggering the PMTs.

The tanks are embedded in snow until the snow level equals the surrounding surface. So at installation there is only snow on the sides, but winds blow snow on top of the tanks. Each year some tanks accumulate up to 30 cm of snow on top while others are still in the original setup without a snow layer. This leads to an asymmetry in the behavior of the array and needs to be understood via data and Monte Carlo comparisons.

1. Note that this is true for 150 tanks. The first 8 installed tanks in the year 2005 and 4 out of 16 tanks installed in the year 2010 are different and contain a Tyvek bag that acts as a reflector.

32ND INTERNATIONAL COSMIC RAY CONFERENCE, BEIJING 2011

Atmospheric Muon Spectrum from Catastrophic Energy Losses in IceCube

THE ICECUBE COLLABORATION[1]
[1]*See special section in these proceedings*

Abstract: While the primary purpose of IceCube is the search for high-energy astrophysical neutrinos, the overwhelming majority of events is caused by downgoing cosmic-ray induced muons. This provides a high-statistics data set which can be used for both detector calibration and supplemental physics investigations. In this work, we present a method to identify TeV-scale catastrophic energy losses along muon tracks and its application to the separation of single high-energy muons from large-multiplicity bundles which dominate the event sample above the horizon at high energies. The information can be used to derive the single-muon energy spectrum at all zenith angles up to energies of hundreds of TeV. We demonstrate that our measurement is sensitive to a cutoff of the proton spectrum at the cosmic ray knee and potentially to the prompt lepton flux caused predominantly by decay of charmed hadrons in atmospheric CR interactions.

Corresponding authors: Patrick Berghaus[2] *(berghaus@icecube.wisc.edu)*, Chen Xu[2] *(chen@udel.edu)*

[2]Bartol Research Institute, University of Delaware, USA

Keywords: Muon Spectrum, Stochastic Losses, Knee

1 Introduction

In recent work on high-energy atmospheric muon fluxes, it was pointed out that second-generation astrophysical neutrino detectors such as IceCube should be able to substantially extend the energy range of muon energy spectrum measurements and hence address various important open problems in cosmic-ray physics. These include verification of hadronic interaction models, primary composition at PeV energies and prompt contributions to the lepton flux [1].

From an experimental perspective, the main challenge in the measurement of the muon energy spectrum is limited spatial resolution due to the sparse instrumentation of the detector. With a minimum separation of 17 meters between Digital Optical Modules (DOMs) in IceCube, resolution of individual muons within a shower is usually impossible. Previous measurements [2, 3] took advantage of the shorter range of large-multiplicity muon bundles compared to individual high-energy muons during passage through matter to measure the muon spectrum at large slant depths near the horizon. The limited angular resolution of the detector and background from up-going atmospheric neutrinos mean that the range of this technique is limited to values up to approximately 100 TeV. Furthermore, the muon spectrum can in this way only be measured in an angular region where the relative contribution from prompt interactions is lowest, excluding investigation of this flux component for practical purposes.

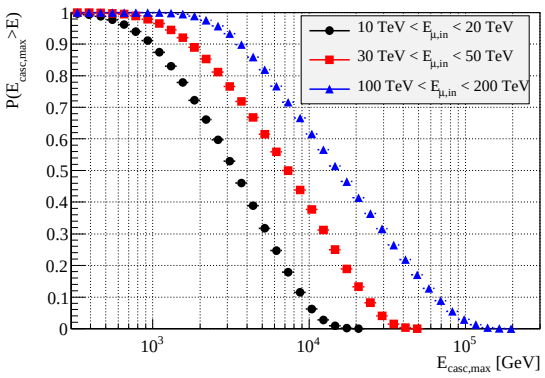

Figure 1: Probability for a stochastic loss above a given energy to occur within the detector volume, for three typical muon energy ranges. The simulation was performed using MMC [5].

In order to take advantage of the full potential of a large-volume detector, it is therefore necessary to develop a method that allows separation of showers with exceptionally highly energetic muons from the dominant background of bundles containing low-energy muons of higher multiplicity. It has long been proposed to make use of the fact that the stochasticity of energy deposition along muon tracks increases with energy [4]. In this analysis, by identifying muon track segments with unusually strong photon

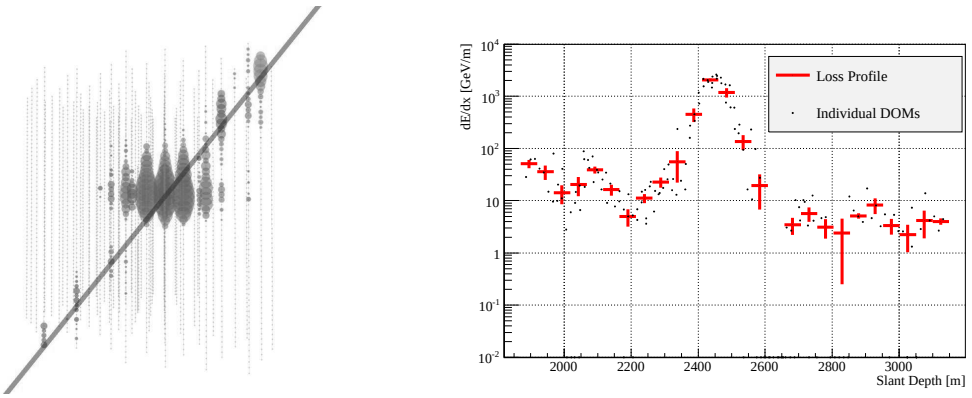

Figure 3: Example for massive stochastic loss event found in IC59 data. The energy deposition estimate shown on the right hand side is consistent with an 80 TeV cascade. The x-axis corresponds to the distance along the track, measured from the surface of the ice.

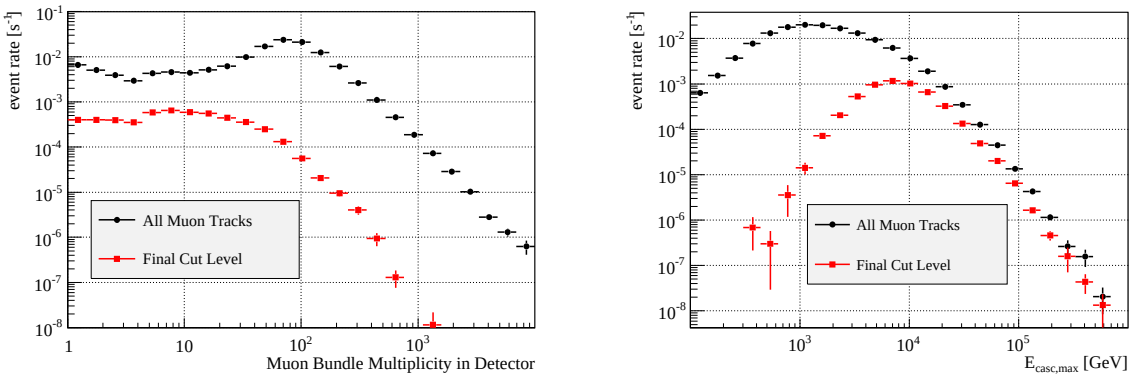

Figure 4: Left: Muon multiplicity in cosmic-ray showers at entry into detector volume before and after selection cuts, simulated using CORSIKA/SIBYLL. The analysis favors muon bundles of moderate multiplicities while reducing both high-multiplicity bundles and low-energy tracks with high recorded DOM charges due to unusual topologies. Right: Effect of selection cuts in dependence of true maximum stochastic loss energy. The effective threshold energy lies around 10 TeV.

- Presence of a well-reconstructed muon track with a length of at least 600 meters inside the detector volume.
- A peak energy loss value in a 50-meter bin along the track which exceeds the median differential energy loss in the event by a factor of 10.
- Location of peak energy loss within 150 meters from at least 50 DOMs, assuring containment within the main detector volume.

Figure 4 shows the cumulative effect of the cuts.

So far, the effective threshold energy for stochastic losses lies around 10 TeV. It is in principle possible to reduce this threshold further by relaxing the requirement on the total recorded DOM charge.

4 Result

To estimate the sensitivity of the method, the measured energy spectrum of stochastic losses was compared to simulations based on various primary composition models [7]:

- **Constant Composition**: The spectrum of each primary nucleus type changes by the same amount at an energy corresponding to the cosmic-ray knee.
- **Rigidity-Dependent Cutoff**: Each component of the cosmic ray flux is subject to a cutoff at an energy that is proportional to the charge of the nucleus.
- **Mass-Dependent Cutoff**: Similar to the previous model, but assuming a cutoff dependent on the nuclear mass. The main distinction here is a sharper transition, resulting in a stronger cutoff signature.
- **No Knee**: This additional model was included for purposes of illustration only, assuming unbroken spectra for each component and therefore completely

32ND INTERNATIONAL COSMIC RAY CONFERENCE, BEIJING 2011

Study of High p_T Muons in IceCube

THE ICECUBE COLLABORATION[1]
[1]*See special section in these proceedings*

Abstract: Muons with a high transverse momentum (p_T) are produced in cosmic ray air showers mostly via semileptonic decay of heavy quarks and the decay of high p_T kaons and pions in jets. These high p_T muons have a large lateral separation from the shower core and accompanying muon bundle. IceCube, a kilometer-scale neutrino telescope consisting of an array of photodetectors buried in the ice of the South Pole and a surface air shower array, is well suited for the detection of high p_T muons. The surface shower array can determine the energy, core location and direction of the cosmic ray air shower while the in-ice array can do the same for the high p_T muon. This makes it possible to measure the cosmic ray muon lateral separation distribution at distances greater than 200 meters. The preliminary results from analysis of data from 25% of the full IceCube detector will be presented.

Corresponding authors: L. Gerhardt[2,3] (*lgerhardt@lbl.gov*), S. R. Klein[2,3] (*SRKlein@lbl.gov*)
[2]*Lawrence Berkeley National Laboratory, Berkeley, California 94720*
[3]*University of California, Berkeley, Berkeley, California 94720*

Keywords: cosmic rays, muons, icecube

1 Introduction

IceCube, a kilometer-scale neutrino telescope, is well suited for measuring the lateral separation of muons in cosmic ray air showers. Completed in December 2010, it consists of a 1 km^3 array of optical sensors (digital optical modules, or DOMs) buried deep in the ice of the South Pole and a 1 km^2 surface air shower array called IceTop. IceTop has an energy threshold of 300 TeV and can reconstruct the direction of showers with energies above 1 PeV within $\sim$1.5° and locate the shower core with an accuracy of $\sim$10 m [1]. The in-ice DOMs (here referred to as IceCube) are buried in the ice 1450 m under IceTop on kilometer-long strings of 60 DOMs with an intra-DOM spacing of 17 m. IceCube can reconstruct high quality tracks of high energy muons with $< 1^\circ$ accuracy. IceTop and IceCube can be used together to select cosmic ray events with a muon with a minimum lateral separation of $\sim$200 m. The measurement of the lateral separation distribution of muons in air showers provides a valuable check on air shower simulation models and can be used as an independent method for determining the cosmic ray composition [2].

The most common source of muons with a large lateral separation is muons with a high transverse momentum (p_T) primarialy from charm and bottom mesons and jets of high p_T partons [2]. The transverse separation is given by:

$$d_T = \frac{p_T h c}{E_\mu} \quad (1)$$

where E_μ is the energy of the high p_T muon, and h is the interaction height of the shower, here taken as an average value of 25 km. The interaction height loosely depends on the composition and a full treatment of this is planned in the future. Using a separation of 200 m (75 meters more than the string separation) as a rough threshold for the two-track resolution distance of the high p_T muon from the shower core gives a minimum resolvable p_T of 8 GeV/c for a 1 TeV muon. Rough calculations predict on the order of tens of high p_T muon events in the studied data sample [2].

The combined acceptance for cosmic ray air showers that pass through both IceTop and IceCube is 0.3 km^{2}sr for the full 86-string IceCube array [3]. By the end of the austral summer of 2006/2007, 22 IceCube strings and 26 IceTop tanks had been deployed. The combined acceptance for showers that trigger both IceTop-26 and IceCube-22 is 0.09 km^{2}sr. In 2007 the discriminator threshold settings for IceTop were changed partway through the year to sub-optimal values, so this analysis discards the data taken during this period leaving 114 days of livetime. A search has been conducted in this data for cosmic ray events with a muon with a large lateral separation.

The underground muon detector MACRO has previously measured the separation between muons in air showers for shower energies ranging roughly from 10^4 GeV to 10^6 GeV [4]. MACRO measured muon pair separations out to a distance of about 65 meters. They verified the linear relationship between p_T and separation shown in Eq. 1 (with a

detector fiducial volume. Further reduction of single muon bundles is done based on the differences in event topologies and timing. For instance, single muon bundles are well-reconstructed by a single track hypothesis, while the high p_T muon events are not. Figure 2 shows the negative log of the reduced likelihood of a single track reconstruction for single muon bundles, and showers with an inserted 8 and 16 GeV/c p_T, 1 TeV muon (separation of 200 m and 400 m from the shower core, assuming an average interaction height of 25 km). Well-reconstructed events have a lower likelihood value on this plot. For large separations, this variable separates single muon bundles from showers which contain a high p_T muon. This analysis retains events with a likelihood greater than 7.5. Next we require that the high p_T muon track be a robust track in the detector with at least 6 direct hits. Finally, the remaining background single muon bundle events are removed by requiring the perpendicular separation between tracks to be at least 160 m. The number of events passing each type of selection criteria for data and simulated background and signal are shown in Table 1.

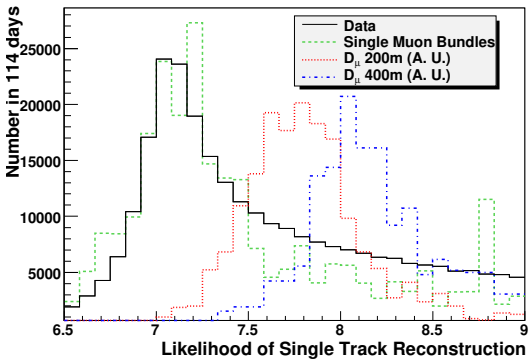

Figure 2: Negative log of the reduced likelihood for the single track reconstruction

4 Results

After applying all selection criteria 53 events remain in 114 days of data. No events remain in the simulated background. One event that passes all the selection criteria is shown in Fig. 3. The reconstructed high p_T muon and bundle track have a perpendicular separation of 207 m at the center of the detector. The two tracks arrive within 470 ns and 3.3° of each other.

4.1 Purity of Final Sample

Simulation of single muon bundle background events is too computationally intensive to accumulate large statistics. Although no simulated single muon bundle event passed all the selection criteria, the possibility exists that some single muon bundle background events could survive in the final data sample. In order to estimate the purity of

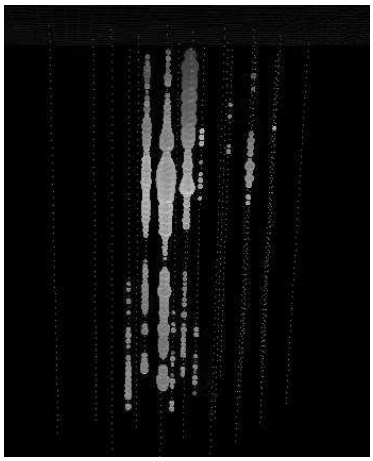

Figure 3: Candidate shower with a high p_T muon. The cosmic ray bundle is on the left and the high p_T muon is on the right.

the final sample a study has been conducted of simulated events which pass the reconstruction quality and double-coincident seleciton criteria (without applying the criteria designed to remove single track events). At this cut level, the only events left in the single muon bundle background are events which are incorrectly split into two tracks by the splitting algorithm. Two previously unused variables were developed that focused on studying how well the bundle fit described the high p_T muon hits and vice versa.

The first variable is the standard deviation of the time residual relative to the reconstructed bundle track (σ_{bundle}). Only hits belonging to the high p_T muon reconstructed track (time residual $<$ 100 ns and distance from the bundle $>$ 90 m) were used to calculate σ_{bundle}. In the single muon bundle background σ_{bundle} is small because the bundle reconstruction is equally good at describing both sets of hits. Conversely, events with high p_T muons have a laterally separated track that is causally disconnected from the bundle track. This leads to larger values of σ_{bundle}.

The second variable is the mean of the time residuals relative to the reconstructed high p_T muon track. Only hits within 90 m of the bundle track are used for this calculation. This variable uses the fact that the parallel but laterally separated high p_T muon track have a negative time residual relative to the bundle track. Single muon bundles incorrectly split into two groups tends to have time residuals that are closer to zero because both groups are causally consistent with the bundle hypothesis.

These two variables are shown in Fig. 4. The background single muon bundles and high p_T muon simulation are at a relaxed cut level with only reconstruction quality and double-coincidence selection criteria applied, while the data points are after all selection criteria have been applied. The dashed grey line is a fit to the mean of the background single muon bundle points. To estimate the purity of the data sample, this line has been moved upwards until every simulated single muon bundle event is below it. Thirty-one

32ND INTERNATIONAL COSMIC RAY CONFERENCE, BEIJING 2011

Searching for PeV gamma rays with IceCube

THE ICECUBE COLLABORATION[1]
[1]*See special section in these proceedings*

Abstract: IceCube and its surface array IceTop can be used to search for PeV gamma rays. At this energy, pair production on the cosmic microwave background limits the gamma ray horizon to a few tens of kiloparsecs. Therefore, the gamma rays have to originate from within the Galaxy, either from the sites of very energetic accelerators or from the interstellar medium and dense molecular clouds, which act as a target for the local cosmic ray flux.

IceCube can efficiently distinguish PeV gamma rays from the background of cosmic rays. For showers within a limited zenith angle range, the in-ice component of IceCube can detect the Cherenkov radiation released by muons that penetrate kilometers deep into the ice while the surface component, IceTop, can measure particles from the same air shower. Gamma-ray air showers have a much lower muon content than cosmic ray air showers of the same energy. IceTop can be used to search for gamma-rays by selecting those showers that lack a signal from a muon bundle in the deep ice.

We investigate the possibility of detecting gamma-ray air showers with IceCube and present results of one year of data, taken in the 2008/2009 season when the detector consisted of 40 strings and 40 surface stations. We derive an upper limit on the ratio of gamma showers to cosmic rays showers of $8.1{\cdot}10^{-4}$ above 1.2 PeV in a region of 10 degrees around the visible part of the Galactic plane. The projected gamma-ray sensitivity of full IceCube, completed at the end of last year, is also studied.

Corresponding author: Stijn Buitink[2,3] (*sbuitink@vub.ac.be*)
[2]*Lawrence Berkeley National Laboratory, Berkeley, USA*
[3]*Interuniversity Institute for High Energy, Vrije Universiteit Brussel, Belgium*

Keywords: Gamma Rays; Galactic Accelerators; Extended Air Showers; IceCube; IceTop

1 Introduction

Gamma rays are an important tool for studying the cosmos; unlike cosmic-rays (CRs), they point back to their points of origin. Air Cherenkov telescopes have detected many high-energy ($E > 1$ TeV) gamma-ray sources. Within our galaxy, gamma-rays have been observed coming from several types of sources: supernova remnants, pulsar wind nebulae, binary systems, and the Galactic center. Extra-galactic sources include Active Galactic Nuclei (AGNs), and other objects containing supermassive black holes. Surface air shower arrays like Milagro have performed all-sky searches for TeV gamma-rays. Although these detectors are less sensitive to point sources than Air Cherenkov telescopes, they have identified several diffuse sources [1].

At higher energies, extra-galactic sources are unlikely to be visible, because more energetic photons are likely to interact with cosmic microwave background radiation (CMBR) photons, and infrared starlight from early galaxies, producing e^+e^- pairs. At 1 PeV, for example, near the peak of the cross-section, photons are limited to a range of about 25 kiloparsecs. It is unknown whether Galactic accelerators exist that can produce gamma rays of such high energy, but an expected flux results from the interaction of CRs with the interstellar medium (ISM).

To date, the best statistics on photons with energies above about 300 TeV come from CASA-MIA, which has set a limit on the fraction of photons in the cosmic-ray flux of 10^{-4}, at energies above 600 TeV [2]. They also set a limit on the relative flux of photons coming from within 5° of the galactic disk of less than 2.4×10^{-5} [3]. This is close to the theoretical expectation due to CR interactions with the ISM. For a Northern hemisphere site like CASA-MIA, the average theoretical prediction is 2×10^{-5} [4]. At somewhat lower energies, gamma-ray emission from the Galactic plane may already have been seen [5].

2 Detection Principle

We select a sample of air showers that are successfully reconstructed by IceTop and have a shower axis that passes through the instrumented area of IceCube deep in the ice. Investigating the muon component of the air showers in the ice allows for CR composition studies. In this analysis, we create a sample of gamma-ray candidates by selecting

32ND INTERNATIONAL COSMIC RAY CONFERENCE, BEIJING 2011

Energy Dependence of the Large Scale Galactic Cosmic Rays Anisotropy Measured With IceCube

THE ICECUBE COLLABORATION[1]
[1] *See special section in these proceedings*

Abstract: We report on a study of the energy dependence in the arrival direction distribution of cosmic rays at median energies of 20 and 400 TeV. The data used in this analysis contain 33×10^9 downward going muon events collected by the IceCube neutrino observatory between May 2009 and May 2010 when it comprised of 59 strings. The high rate of cosmic ray induced muons observed by IceCube allows us to perform the first study of the galactic cosmic ray arrival distribution around 400 TeV in the Southern sky. The sidereal anisotropy observed at 400 TeV shows substantial differences with respect to that at lower energy. Studies of the energy dependence of the anisotropy could further enhance the understanding of the structure of the local interstellar magnetic field and possible nearby cosmic ray sources.

Corresponding Authors: Rasha Abbasi[2] (*rasha.abbasi@icecube.wisc.edu*), Paolo Desiati[2] (*desiati@icecube.wisc.edu*)
[2] *Dept. of Physics, University of Wisconsin-Madison, Madison, WI 53703, USA*

Keywords: IceCube, Cosmic Rays, Anisotropy, Muons, Neutrinos.

1 Introduction

During the last decades, Galactic cosmic rays have been found to have a small but measurable energy dependent sidereal anisotropy in their arrival direction distribution with a relative amplitude of order of 10^{-4} to 10^{-3}. The first comprehensive observation of the cosmic ray sidereal anisotropy was provided by a network of muon detectors sensitive to cosmic rays between 10 and several hundred GeV [1]. More recent underground and surface array experiments in the Northern hemisphere have shown that a sidereal anisotropy is present in the TeV energy range (i.e. Tibet Air Shower Arrays (Tibet ASγ) [2], Milagro [3]). The IceCube neutrino observatory reported for the first time the observation of the cosmic rays sidereal anisotropy in the Southern sky at energies in excess of about 10 TeV [4]. The cosmic ray anisotropy reported by IceCube showed that the large scale features were a continuation of those observed in the Northern hemisphere in the same energy range.

At high energies, the Tibet ASγ collaboration reported the non-observation of a sidereal anisotropy in the cosmic ray arrival direction distribution at $\sim$ 300 TeV [2]. Another measurement at $\sim$370 TeV was recently published by the EAS-TOP collaboration reporting a larger sidereal anisotropy in amplitude with a shift in phase from that observed at lower energies [5]. At this point the two observations do not provide a coherent picture of the sidereal anisotropy at high energy in the Northern hemisphere.

In this contribution we present the analysis and the results of the study of large scale cosmic ray anisotropy at median energies of 20 and 400 TeV by IceCube for the Southern celestial sky. Observations of the energy dependence of the anisotropy could provide us with further information for the development of theoretical models to better understand the origin and propagation of cosmic rays.

2 Data Analysis

The main goal of the IceCube neutrino observatory is to detect astrophysical neutrinos. Neutrinos passing through the Earth and interacting in the vicinity of IceCube produce muons or other secondaries that emit Cherenkov radiation in the clear ice surrounding the detector. It is these light signals that the IceCube optical modules record. On the other hand, muons produced by cosmic ray air-showers in the atmosphere above IceCube are also detected. These are observed as down-going tracks.

The data used in this analysis are the downward going muons collected by the IceCube detector comprising 59 strings. The data were collected from May 2009 to May 2010 [6]. The events used in this analysis are those reconstructed by an online likelihood based reconstruction algorithm at an average rate of $\sim$1250 Hz with a median

The sidereal distribution of relative intensity in the arrival direction of the cosmic rays for the low and high energy samples are used to evaluate the spread in the experimental observation from the full-year event samples. The gray bands in the right ascension projection in Figures 1 and 2 describe the maximal spread obtained from the result of all the stability checks described in this section.

4.1.2 Solar Diurnal Anisotropy

To test for the stability of the observatory and its time coverage, an effective way to have an absolute calibration of the experimental sensitivity for the detection of the sidereal directional asymmetries is to measure the solar anisotropy from the Earth's revolution around the Sun. This observation has solid theoretical grounds and it was first reported in 1986 [11] and then later observed by multiple experiments in the multi-TeV energy range (i.e. [2], [3]). The observed solar anisotropy is consistent with a dipole that describes an apparent excess of cosmic rays in the direction of Earth's motion around the Sun and a deficit in the opposite direction.

Figure 3 shows the projections of the cosmic ray arrival direction in solar reference frame, for both energy samples (20 and 400 TeV). The error bars are the statistical errors, and the shaded bands indicate the expectation of the dipole. A fit to the projection of relative intensity distribution is shown by the black line and was done using the first harmonic term of eq. (1). The figures show that the experimental observation of the solar dipole is consistent with the expectations in both amplitude and phase. This observation of the solar diurnal anisotropy supports the reliability of the sidereal anisotropy determination.

4.1.3 Anti-sidereal Anisotropy

An annual modulation in the amplitude of the solar anisotropy is expected to result in a spurious effect in the sidereal anisotropy. This would produce a bias in the observed sidereal anisotropy. To estimate this bias the so-called anti-sidereal time, i.e. a non-physical time frame obtained by reversing the sign of the transformation from solar time to sidereal time [12].

Figure 4 shows the projections of the cosmic ray arrival direction in anti-sidereal reference frame, for both energy samples (20 and 400 TeV). The error bars are the statistical errors. The distributions were then fitted to the dipole term of eq. (1). The uncertainty in the first harmonic amplitude and phase implied by the study in the anti-sidereal time frame is within the statistical and systematic errors determined from the data stability tests. The absence of the signal in the anti-sidereal time insures the reliability of the anisotropy observed in sidereal time.

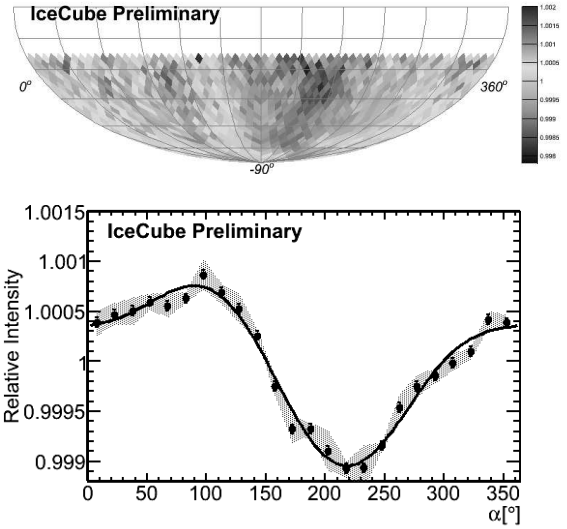

Figure 1: The top figure is the IceCube relative intensity cosmic ray map for the low energy sample (Median energy of the primary cosmic ray particle of 20 TeV). The bottom figure is the one dimensional projection in right ascension α of the two-dimensional cosmic ray map. The black line corresponds to the first and second harmonic fit to the data. The gray band indicates the estimated maximal systematic uncertainties.

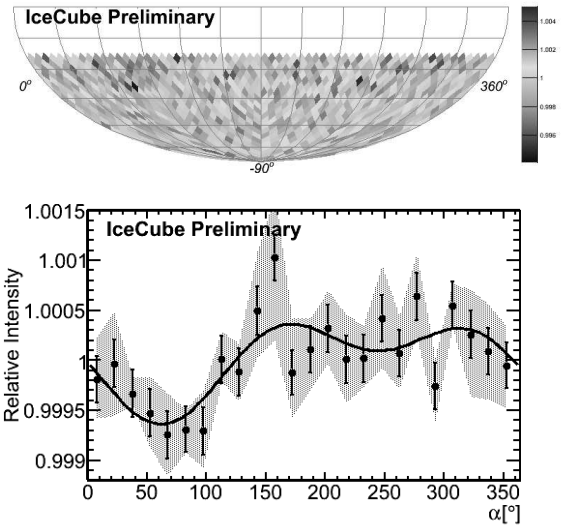

Figure 2: The top figure is the IceCube relative intensity cosmic ray map for the high energy sample (Median energy of the primary cosmic ray particle of 400 TeV). The bottom figures is the one dimensional projection in right ascension α of the two-dimensional cosmic ray map. The black line corresponds to the first and second harmonic fit to the data. The gray band indicates the estimated maximal systematic uncertainties.

5 Conclusion

In this contribution we presented the results on the large scale cosmic ray sidereal anisotropy at cosmic ray median

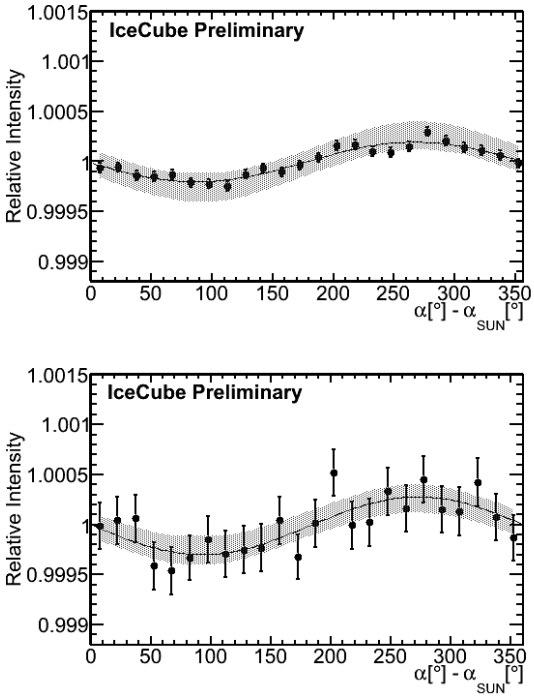

Figure 3: The solar projections for cosmic rays with median energy of 20 TeV (The top figure) and 400 TeV (The bottom figure). The error bars are the statistical errors, and the shaded band indicated the solar diurnal dipole expected from the motion of the Earth around the Sun.

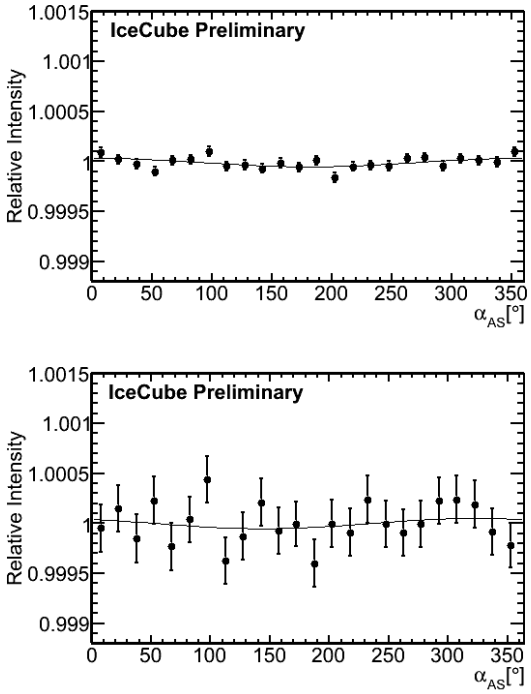

Figure 4: The anti-sidereal projections for cosmic rays with median energy of 20 TeV (The top figure) and 400 TeV (The bottom figure). The error bars are the statistical errors. The black line corresponds to the first harmonic fit to the data.

energies of 20 TeV and 400 TeV. The source of the sidereal anisotropy is still unknown. It is believed that a possible contribution to this observed anisotropy might be from the Compton-Getting effect, due to the orbital motion of the solar system around the galactic disk. However, the sidereal anisotropy from both energy samples do not appear to be consistent with that expected from the suggested Compton-Getting model neither in amplitude nor in phase.

The sidereal anisotropy observed at 20 TeV with IceCube-59 is consistent with the previously reported observation with IceCube [4], thus providing a confirmation of an apparent continuation of the arrival distribution pattern observed in the Northern hemisphere. On the other hand the sidereal anisotropy observed at 400 TeV shows substantial differences with respect to that at lower energy. The anisotropy at high energy shows a relative deficit region in right ascension where the broad excess dominated at primary median energy of 20 TeV. Also the wide relative deficit region at low energy seemed to have disappeared at primary median energy of 400 TeV. Whatever generated the sidereal anisotropy at 20 TeV seems to have no effect at 400 TeV.

This is the first observation of the sidereal anisotropy at 400 TeV in the Southern hemisphere. We are continuously analyzing events from IceCube with updated configurations. IceCube construction is now completed with 86 strings deployed with a volume of km^3 in January of 2011. With the higher statistical power expected from the observed cosmic ray muons we will be able to improve our understanding of the energy dependence of the anisotropy with more significance and close to the knee region. The energy dependence of the cosmic ray anisotropy is vital to our understanding of the source and propagation of cosmic rays.

References

[1] Nagashima et al., J. Geophys. Res., 1998, **103**: 17429.
[2] Amenomori et al., Science, 2006, **314**:439.
[3] Abdo et al., Astrophys. J., 2009, **698**:2121.
[4] Abbasi et al., Astrophys. J., 2010, **718**:L194.
[5] Aglietta et al., Astrophys. J., 2009, **692**:130.
[6] Abbasi et al., arXiv:1105.2326.
[7] Bercovitch, M., et al., International Cosmic Ray Conference,1981, **67**: 246.
[8] Cutler, D. J., et al., Astrophys. J., 1991, **376**: 322.
[9] Andreyev, Y. M., et al., International Cosmic Ray Conference, 1987, **2**: 22.
[10] Munakata, K., et al., International Cosmic Ray Conference,1999, **7**: 293.
[11] Cutler, D. J., & Groom, D. E., Nature, 1986,**322**: 434.
[12] Farley, F. J. M., & Storey, J. R., Proc. Phys. Soc., 1954,**67**: 996.
[13] Redfield, S., & Linsky, J. L., Astrophys. J., 2000,**534**: 825.

32ND INTERNATIONAL COSMIC RAY CONFERENCE, BEIJING 2011

Observation of Anisotropy in the Arrival Direction Distribution of Cosmic Rays at TeV Energies with IceCube

THE ICECUBE COLLABORATION[1]
[1]*See special section in these proceedings*

Abstract: The IceCube neutrino detector at the South Pole is sensitive to atmospheric muons produced by primary cosmic rays in the TeV energy range. The high rate of events (about 2 kHz in the full 86-string detector) allows for searches of anisotropy in the arrival direction distribution of cosmic rays at the level of a few parts per mille. Using the muon data recorded with IceCube between 2007 and 2010, we show that the cosmic ray flux in the southern hemisphere is not isotropic, but exhibits significant structure on multiple angular scales. In addition to large-scale features in the form of strong dipole and quadrupole moments, the data include several localized regions of excess and deficit on scales between 10° and 30°. These features are statistically significant. The origin of the features is currently unknown.

Corresponding Authors: Segev BenZvi[2] (*sybenzvi@icecube.wisc.edu*),
Marcos Santander[2] (*santander@icecube.wisc.edu*), Simona Toscano[2] (*toscano@icecube.wisc.edu*),
Stefan Westerhoff[2] (*swesterhoff@icecube.wisc.edu*)
[2]*Dept. of Physics, University of Wisconsin-Madison, Madison, WI 53703, USA*

Keywords: Cosmic Rays – TeV; Anisotropy; Muons; Neutrinos

1 Introduction

The IceCube detector, deployed between 1450 m to 2450 m below the surface of the South Polar ice sheet, is designed to detect upward-going neutrinos from astrophysical sources. However, it is also sensitive to downward-going muons from cosmic-ray air showers. To penetrate the ice and trigger the detector, the muons must be produced by cosmic rays with energies of at least several TeV. The arrival direction of a cosmic muon is typically within 0.2° of the direction of the primary particle, so the arrival direction distribution of muons is also a map of cosmic ray arrival directions between about 1 and several hundred TeV.

At energies of a few TeV, it is believed that galactic magnetic fields should randomize the arrival directions of charged cosmic rays. However, in recent years an anisotropy in the arrival direction distribution has been reported on both large and small angular scales. The anisotropy is observed in the northern sky between several TeV and several hundred TeV by the Tibet ASγ array [1], Super-Kamiokande [2], Milagro [3, 4], ARGO-YBJ [5], and EAS-TOP [6]. In 2010, an analysis of muons recorded by the IceCube detector also revealed a large-scale anisotropy in the southern sky [7]. In these proceedings, we present the results of a search of the southern sky for anisotropy on all angular scales using data recorded between May 2009 and May 2010.

2 The IceCube Detector and Data

IceCube is a km^3-size neutrino detector frozen into the glacial ice sheet at the geographic South Pole. High-energy charged particles passing through the detector emit Cherenkov radiation, and their tracks are recorded by an array of Digital Optical Modules (DOMs) embedded in the ice. The DOMs are attached to 86 vertical cables, or strings (with 60 DOMs per string), which are used to transmit data to the surface. Construction of IceCube was completed in December 2010. The detector has been operating in various configurations since construction began. Between 2007 and 2008, it was operated with 22 strings deployed (IC22), between 2008 and 2009 with 40 strings (IC40), and between 2009 and 2010 with 59 strings.

Muons are identified using a simple majority trigger, which requires 8 or more DOMs in local coincidence within a $5\ \mu$s window. The trigger rate of downgoing muons is 0.5 kHz in IC22, 1.2 kHz in IC40, and 1.4 kHz in IC59, about a factor of 10^6 larger than the neutrino rate. The rate is too large to transfer complete waveforms for all events via satellite, so the muon data are reconstructed on-line and compressed using a Data Storage and Transfer (DST) format. Muon tracks are identified using a maximum-likelihood reconstruction, and the event arrival direction and energy estimators are stored in DST files and sent north by satellite. Digitized waveforms are discarded due to limited bandwidth.

The analysis presented in this paper uses the DST data collected during IC59 operations between May 20, 2009 and May 30, 2010. The data set contains nearly 3.4×10^{10} muon events recorded during a live time of 335.5 days. A cut in zenith angle at 65° removes less well-reconstructed tracks near the horizon, reducing the final analysis sample to 3.2×10^{10} events. The median angular resolution of events in the sample is 3°; unlike the neutrino analysis, the cuts have not been optimized for point source identification. Using simulated data, we estimate the median energy of the events to be 20 TeV. The energy resolution of the cosmic ray primaries is about $\Delta \log (E/\mathrm{eV}) = 0.5$.

3 Analysis

3.1 Calculation of the Reference Level

The arrival direction distribution of cosmic rays in IceCube exhibits anisotropy caused by non-physical effects such as gaps in the detector uptime. These effects must be removed before any physical anisotropy can be identified. Therefore, the first step in the analysis is the creation of a "reference map," a sky map that describes what the arrival direction distribution would be if the cosmic ray flux were isotropic. The reference map must be subtracted from the arrival direction distribution in the data to find regions where the cosmic ray flux deviates from the isotropic expectation.

We estimate a reference map for IC59 data using the time-scrambling method of Alexandreas et al. [8]. The sky is binned into an equal-area grid in equatorial coordinates with 0.9° resolution using the publicly-available HEALPix library [9]. From this sample two sky maps are produced. The data map $N(\alpha, \delta)$ stores the arrival directions of all events. For each detected event in the data map, "fake" events are generated by keeping the local zenith and azimuth angles (θ, ϕ) fixed but reassigning the time to that of another event recorded within a pre-defined time window Δt. The event times within the window are resampled 20 times and used to generate 20 fake celestial coordinate pairs (α, δ) which are used to fill a reference sky map $\langle N(\alpha, \delta) \rangle$ with a weight of 1/20.

A known disadvantage of the method is that it can be biased by a strong anisotropy, leading to artificial deficits or excesses next to regions of true excess or deficit [3]. However, the procedure does preserve the local arrival direction distribution of the data and naturally compensates for variations in the event rate which are difficult to model, such as changes in atmospheric conditions which affect the production of muons in air showers. The only critical requirement for time scrambling is to choose the buffer length Δt such that detector conditions remain stable during this period. Using χ^2 tests to compare the distribution of arrival directions in local coordinates across measurement periods, we have verified that the IceCube detector is stable over periods of at least one full day. In this analysis we choose $\Delta t = 24$ hr.

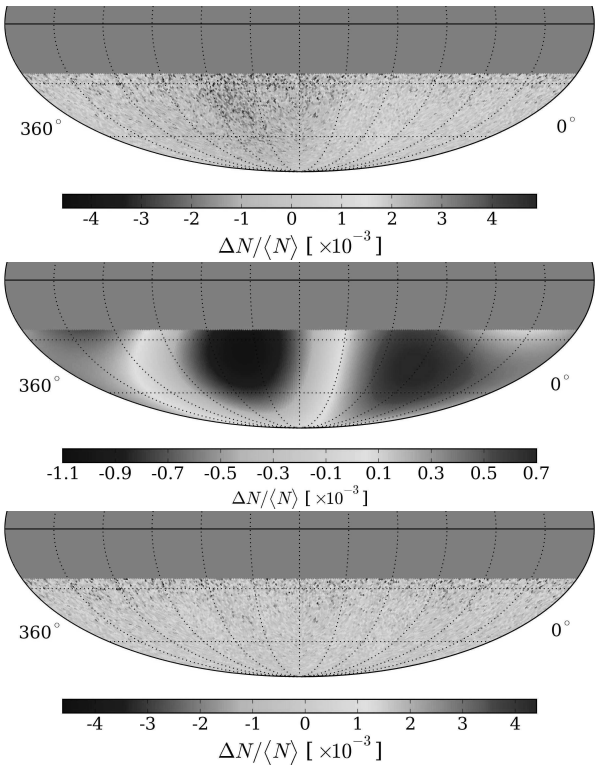

Figure 1: *Top*: Relative intensity of the IC59 data produced with $\Delta t = 24$ hr. *Middle*: Fit of dipole and quadrupole moments to the relative intensity. *Bottom*: Residual map after removal of the dipole and quadrupole.

3.2 Relative Intensity

Once the data and reference maps are calculated, deviations from isotropy can be analyzed by computing the relative intensity

$$\frac{\Delta N_i}{\langle N \rangle_i} = \frac{N_i(\alpha, \delta) - \langle N_i(\alpha, \delta) \rangle}{\langle N_i(\alpha, \delta) \rangle}. \quad (1)$$

which gives the amplitude of deviations from the isotropic expectation in each angular bin i. The significance of the deviation in bin i can be calculated using the method of Li and Ma [10].

A map of relative intensity of the IC59 data, binned with 0.9° resolution, is shown at the top of Fig. 1. The map exhibits obvious correlations between bins, such as a broad excess in the relative counts near $\alpha = 105^\circ$ and a broad deficit near $\alpha = 225^\circ$. The relative intensity in these regions is of order 10^{-3}. This structure is the large-scale anisotropy reported in the IC22 data by Abbasi et al. [7]. Since the IC59 data set is larger than that of IC22 by an order of magnitude, it is possible to see the large-scale structure in the data without further rebinning.

3.3 Removal of Large-Scale Structure

The relative intensity shown at the top of Fig. 1 is dominated by large-scale structures, but there are additional

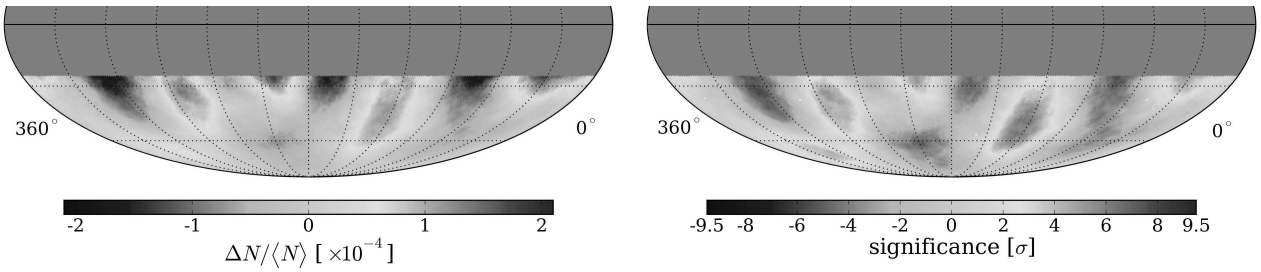

Figure 2: IC59 residual maps after subtraction of dipole and quadrupole moments, showing relative intensity (left) and significance before trial factors are applied (right). The maps have been smoothed with a circular window of 20°.

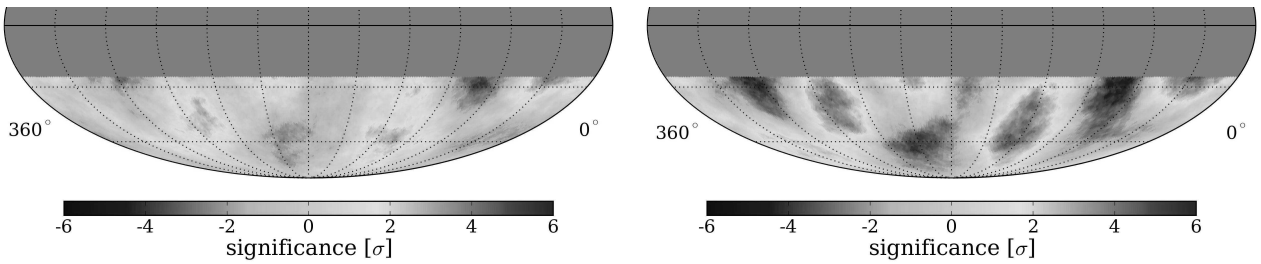

Figure 3: Residual maps from IC22 (left) and IC40 (right) showing the significance of deficit and excess regions with 20° smoothing.

small-scale features in the map. This can be demonstrated by calculating the angular power spectrum of the data, which exhibits significant power not only at the largest angular scales, but also down to scales of about 10° (see detailed discussion in Abbasi et al. [11]).

We can also demonstrate the presence of small-scale structure by explicitly removing the largest angular correlations in the data. This is accomplished by fitting dipole and quadrupole terms to the relative intensity map and then subtracting the fit to obtain a map of residual counts. In the middle panel of Fig. 1, we show the result of the fit of dipole and quadrupole moments to the intensity map. By themselves, these two terms account for much of the amplitude of the per-mille anisotropy observed in the data. However, the fit $\chi^2/\text{ndf} = 14743/14187$ corresponds to a χ^2-probability of approximately 0.05%, suggesting that the dipole and quadrupole are not sufficient to explain all of the structures observed in the angular distribution of $\Delta N/\langle N\rangle$.

Subtraction of the dipole and quadrupole fit from the data gives the bottom panel in Fig. 1. The fit residuals are relatively featureless at first glance, but the bin size is not optimized for a study of significant anisotropy at angular scales larger than the angular resolution of the detector. To increase the sensitivity to the small-scale structure in the data, we apply a smoothing procedure which takes the reference level and residual data counts in each bin and adds the counts from pixels within some angular radius of the bin. This procedure results in a map with Poisson uncertainties, though the bins are no longer statistically independent.

Smoothed residual maps of relative intensity and significance are shown in Fig. 2. To make this figure, a smoothing radius of 20° was chosen. Strong regions of excess and deficit are visible in the data. Note that the actual size of any given excess or deficit region (and thus the optimal smoothing scale) is not known *a priori.* Therefore, we study the sky map on all smoothing scales from 3° (the angular resolution of the data) to 45° in steps of 1° and search for regions of high significance at any location.

Applying this procedure, the two most significant features on the sky are a region with a peak significance of 5.3σ at a smoothing radius of 22° ($\alpha = 122.4^\circ, \delta = -47.4^\circ$) and a region of peak significance 4.9σ at a smoothing radius of 13° ($\alpha = 263.0^\circ, -44.1^\circ$). The significance values account for statistical trials due to the scan over smoothing radii and the location of the most significant pixels. The trial factors were estimated using a Monte Carlo simulation of an isotropic flux recorded by the IceCube detector.

4 Systematic Checks

Several tests have been performed on the data to ensure the stability of the observed anisotropy and to rule out possible sources of systematic bias. Among the influences that might cause spurious non-physical anisotropies are the detector geometry, the detector livetime, non-uniform exposure of the detector to different regions of the sky, and diurnal and seasonal variations in atmospheric conditions. Due to its unique location at the South Pole, many of these effects play a lesser role for IceCube than for detectors at the middle latitudes. We check the validity of this assumption by searching the data for a signal expected in solar coordinates, and by examining the data from previous configurations of the detector.

32ND INTERNATIONAL COSMIC RAY CONFERENCE, BEIJING 2011

Measurement of the Solar Anisotropy with IceCube

THE ICECUBE COLLABORATION[1]
[1]*See special section in these proceedings*

Abstract:

IceCube is a kilometer scale neutrino observatory that collects a large number of cosmic ray induced muon events. These events, which are background for neutrino searches, are observed at a rate that is suitable for high-statistics studies of cosmic rays in the Southern hemisphere. The apparent anisotropy created by the motion of the Earth around the Sun, the solar dipole, is systematically analyzed. The solar dipole is simulated, and the predictions for the integrated effect over an entire year and over shorter periods of a quarter-year are compared to data. The experimental observation is found to be in good agreement with the expectation. Finally, we show that the interference between the solar dipole and the sidereal anisotropy is well understood within the statistical uncertainties.

Corresponding Authors: Craig Price[2] (*cprice@icecube.wisc.edu*), Rasha Abbasi[2] (*rasha.abbasi@icecube.wisc.edu*), Paolo Desiati[2] (*paolo.desiati@icecube.wisc.edu*)
[2]*Dept. of Physics, University of Wisconsin-Madison, Madison, WI 53703, USA*

Keywords: IceCube; Cosmic Rays; Anisotropy; Muons; Neutrinos

1 Introduction

The motion of an observer in the cosmic ray plasma is predicted to cause an apparent dipole effect in the cosmic ray arrival direction; this effect was first pointed out in 1935 by Arthur Compton and Ivan Getting [1]. Using this principle, the motion of the Earth around the Sun would produce an excess in the direction of motion and a deficit in the opposite direction. This observation was first reported by Cutler in 1986 [2], and then later observed by multiple experiments (i.e. Tibet Air Shower Arrays (Tibet ASγ) [3], Milagro [4], and EAS-TOP [5]). This measurement is referred to in this contribution as the solar dipole effect anisotropy and is expressed as

$$\frac{\Delta I}{\langle I \rangle} = (\gamma + 2)\frac{v}{c}\cos(\theta_v) \qquad (1)$$

where I is the intensity, γ is the differential cosmic ray spectral index, v is the Earth's velocity, c is the speed of light, and θ_v is the angle between the reconstructed arrival direction of the cosmic rays and the direction of the motion of the Earth [6].

In addition to the solar dipole effect, galactic cosmic ray anisotropies have been observed by underground and surface array experiments in the Northern hemisphere such as Tibet ASγ [3]. Furthermore, IceCube recently reported the first observation of the sidereal anisotropy in cosmic ray arrival direction in the Southern sky [7] with a relative amplitude of the order of 10^{-4} to 10^{-3}. The cosmic ray anisotropy showed that the sidereal anisotropy in the Southern sky is a continuation of that observed in the Northern hemisphere.

In this proceeding, we report on the study of the observation and the expectation of the solar dipole effect in one full year. We also examine the effect of the mutual interference between the sidereal anisotropy and the solar dipole effect by examining quarter-year periods. The solar dipole effect and the interference between the sidereal and the solar effect over quarter-year periods is found to be well understood. This understanding supports the reliability of the sidereal anisotropy observations.

2 Data Analysis

IceCube is optimized for the detection of up-going, high-energy neutrinos, however its trigger rate is dominated by down-going atmospheric muons created in cosmic ray air-showers above the detector. In this work, we use the down-going atmospheric muon flux as our signal to study cosmic rays in the Southern sky. The data used in this analysis are the down-going muons collected by the IceCube detector in its 59-string configuration from May 2009 to May 2010. The data are reconstructed by an online maximum likelihood based reconstruction algorithm at an average rate of $\sim$1.2 kHz. A range of selection criteria is applied to the data to ensure detector stability. The final data set consists

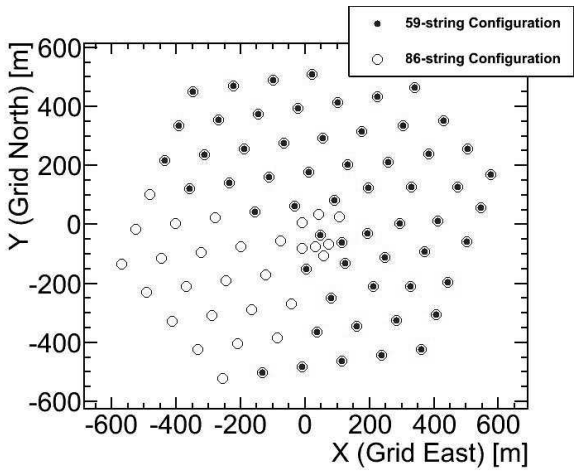

Figure 1: This plot shows the IceCube configuration with 86 strings in empty circles and the 59-string configuration in filled circles.

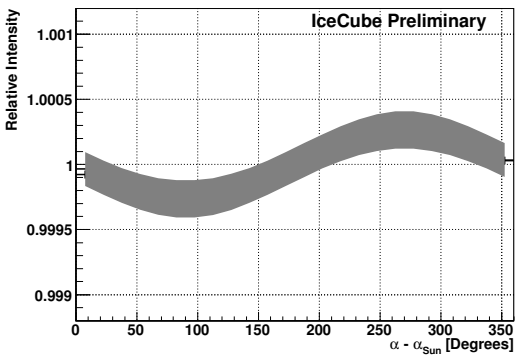

Figure 2: The plot shows the one-dimensional projection in $\alpha - \alpha_{Sun}$ of the relative intensity of cosmic rays. The data are shown with statistical uncertainties in black crosses, and the black line corresponds to the expectation from eq. 1. The gray shaded band indicates the 68% spread of the uncertainty in the simulated solar dipole.

of 33 billion events and corresponds to a detector livetime of 324.8 days. The events are initiated by muons from cosmic ray air-showers with a median primary energy of 20 TeV. The angular resolution between the muon to the primary cosmic ray particle has a median value of $\sim 3^\circ$.

Located at the South Pole, IceCube observes the Southern sky year-round. However, an artificial azimuthal asymmetry occurs as an artifact of the detector's geometrical configuration (Figure 1) combined with non-uniform time coverage. This azimuthal asymmetry was eliminated by reweighting the azimuthal arrival directions of the incoming cosmic rays [7].

3 Solar Dipole Anisotropy Measurement and Expectation

The solar dipole is a well-known signal, both from theory and from observations by other experiments. A measurement of this well-known signal with IceCube strongly supports the reliability of the observation of the sidereal anisotropy with the same detector [8].

The amplitude of the solar dipole depends on the geographical latitude of the observer and on the angular distribution of the detected cosmic ray events at the observatory. Due to the location of the IceCube Observatory at the South Pole, the sky is fully visible at any given time. Therefore, the solar dipole is observed in a reference system where the location of the Sun is fixed, where the latitude coordinate is the declination, and the longitude coordinate is defined to be the difference between the right ascension of the cosmic ray arrival direction and the right ascension of the Sun ($\alpha - \alpha_{Sun}$). In this reference frame, the excess due to the solar dipole is expected to be at 270° and a deficit at 90°.

To verify that the experimental observation of the solar dipole is consistent with the expectation, the predicted projection of the solar anisotropy was calculated for the IceCube location. Since the observed amplitude of the solar dipole depends on the actual angular distribution of the detected muon events, the calculation of the expectation was performed using the azimuth-corrected experimental data. The expectation of the solar dipole was calculated by computing the relative intensity of the solar dipole through the cosmic ray plasma (through eq. 1). Instead of counting the number of events within a given bin in right ascension from the Sun, we calculated for each event, a mean weight corresponding to the expected relative intensity of the solar dipole.

The uncertainties in the cosmic ray spectral index, in the Earth's velocity, and in the reconstructed arrival direction of the events were included into the calculation of the uncertainty of the expectation. The mean spectral index was evaluated using the all-particle cosmic ray spectrum from [9] and was found to be 2.67 $\pm$ 0.19. The value used for Earth's velocity was v = 29.8 $\pm$ 0.5 km/s, where the error takes into account the spread between the maximum and minimum along the elliptical orbit. The angle θ_v between the reconstructed direction of the muon events and the Earth's velocity vector at the time the event was detected was evaluated accounting for the experimental point spread function. The expected solar dipole distribution, including the 68% spread in the uncertainty of the expectation, is shown in Figure 2. This figure shows that the observation is consistent with the expectation in both amplitude and phase.

32ND INTERNATIONAL COSMIC RAY CONFERENCE, BEIJING 2011

Study of Forbush Decreases with IceTop

THE ICECUBE COLLABORATION[1]
[1]*See special sections in these proceedings*

Abstract: IceTop, the surface component of the IceCube neutrino observatory, is an air shower array installed at the Amundson-Scott South Pole station. It consists of 162 ice Cherenkov detectors, each 90 cm deep with surface area 2.7 m^2. The tanks detect secondary particles produced by cosmic rays interacting in the atmosphere with a counting rate exceeding 1 kHz per detector. The statistical precision enabled by the high counting rate of the array enables the study of cosmic ray heliospheric disturbances with unprecedented time resolution in the multi-GeV energy regime. Since the detector has each different threshold settings, it is also possible to estimate the energy spectrum of particles in such events. We illustrate the performance during a Forbush decrease observed in February, 2011.

Corresponding authors: Takao Kuwabara[2] (*takao@bartol.udel.edu*), Paul Evenson[2] (*evenson@udel.edu*)
[2]*Bartol Research Institute and Dept. of Physics and Astronomy, University of Delaware, Newark, DE 19716, U.S.A.*

Keywords: IceCube, IceTop, Forbush decrease

1 Introduction

IceTop, the surface component of the IceCube neutrino observatory, is located at the Amundson-Scott station near the geographic South Pole (altitude 2835m). It is an air shower array consisting of 162 ice Cherenkov detectors, each 90 cm deep with surface area 2.7 m^2. Signals are recorded by photomultipliers in two Digital Optical Modules (DOMs) frozen into the ice in each detector. Two DOMs in a detector are typically operated at high and low gain settings to provide appropriate dynamic range. In this paper we consider only data from the set of 146 "high gain" DOMs that were deployed prior to the 2010-11 austral summer. The large detector volume coupled with the high altitude and nearly zero geomagnetic cutoff at the South Pole yield an extremely high counting rate that allows the study of cosmic ray time variations with unprecedented accuracy.

This analysis uses counting rates from the two discriminators in the high gain DOMs. They are termed SPE (Single Photo Electron), and MPE (Multi Photo Electron) for historical reasons. The SPE discriminators are actually set to thresholds ranging between 1 and 20 photoelectrons whereas the MPE threshold are all set near 20 photoelectrons. The counting rates at those SPE and MPE threshold settings range from 1 to 10 kHz. IceTop detectors respond to several components of the secondaries (muons, neutrons, and electomagnetic components [1]) produced by interactions of $>$0.6 GeV primary cosmic rays with Earth's atmosphere, and the signal spectrum of the detector contains information on the spectrum of the primary particles. By observing the intensity variation at different threshold settings we can estimate the energy spectrum of primary particles during the heliospheric events.

At energies up to $\sim$100 GeV, primary galactic cosmic rays experience significant variations in response to passing solar wind disturbances such as interplanetary coronal mass ejections (ICMEs). ICMEs consist of large eruptions of magnetic field and plasma from Sun. ICMEs accompanied by a strong shock often have a depleted region of galactic cosmic rays behind the shock and within the CME. When Earth enters this depleted region, ground-based cosmic ray detectors record a "Forbush Decrease" [2]. During the decrease the cosmic ray intensity fluctuates in response to magnetic structures embedded in the ICME. Data with high statistical precision from IceTop allow study of these structures with unprecedented time resolution, coupled with simultaneous spectral information. In this paper, we illustrate the performance of IceTop during a Forbush decrease event observed on 18 February 2011.

2 Observation of 18 February 2011 Forbush Decrease

The 18 February 2011 Forbush decrease, related to the X2.2 solar flare that occurred on 15 February 01:44 UT, was the largest Forbush decrease since December 2006. A summary of observations of this decrease is shown in Figure 1. The four top panels display solar wind speed, total component (Bt) and North-South component (Bz) of